Novel Mouse Xenograft Models Reveal a Critical Role of CD4$^+$ T Cells in the Proliferation of EBV-Infected T and NK Cells

Ken-Ichi Imadome[1☯*], Misako Yajima[1☯¤], Ayako Arai[2], Atsuko Nakazawa[3], Fuyuko Kawano[1], Sayumi Ichikawa[1,4], Norio Shimizu[4], Naoki Yamamoto[5¤], Tomohiro Morio[6], Shouichi Ohga[7], Hiroyuki Nakamura[1], Mamoru Ito[8], Osamu Miura[2], Jun Komano[5], Shigeyoshi Fujiwara[1*]

1 Department of Infectious Diseases, National Research Institute for Child Health and Development, Tokyo, Japan, **2** Department of Hematology, Tokyo Medical and Dental University, Tokyo, Japan, **3** Department of Pathology, National Center for Child Health and Development, Tokyo, Japan, **4** Department of Virology, Division of Medical Science, Medical Research Institute, Tokyo Medical and Dental University, Tokyo, Japan, **5** AIDS Research Center, National Institute of Infectious Diseases, Tokyo, Japan, **6** Department of Pediatrics and Developmental Biology, Tokyo Medical and Dental University, Tokyo, Japan, **7** Department of Perinatal and Pediatric Medicine, Graduate School of Medical Sciences, Kyushu University, Fukuoka, Japan, **8** Central Institute for Experimental Animals, Kawasaki, Japan

Abstract

Epstein-Barr virus (EBV), a ubiquitous B-lymphotropic herpesvirus, ectopically infects T or NK cells to cause severe diseases of unknown pathogenesis, including chronic active EBV infection (CAEBV) and EBV-associated hemophagocytic lymphohistiocytosis (EBV-HLH). We developed xenograft models of CAEBV and EBV-HLH by transplanting patients' PBMC to immunodeficient mice of the NOD/Shi-*scid*/IL-2Rγ^{null} strain. In these models, EBV-infected T, NK, or B cells proliferated systemically and reproduced histological characteristics of the two diseases. Analysis of the TCR repertoire expression revealed that identical predominant EBV-infected T-cell clones proliferated in patients and corresponding mice transplanted with their PBMC. Expression of the EBV nuclear antigen 1 (EBNA1), the latent membrane protein 1 (LMP1), and LMP2, but not EBNA2, in the engrafted cells is consistent with the latency II program of EBV gene expression known in CAEBV. High levels of human cytokines, including IL-8, IFN-γ, and RANTES, were detected in the peripheral blood of the model mice, mirroring hypercytokinemia characteristic to both CAEBV and EBV-HLH. Transplantation of individual immunophenotypic subsets isolated from patients' PBMC as well as that of various combinations of these subsets revealed a critical role of CD4$^+$ T cells in the engraftment of EBV-infected T and NK cells. In accordance with this finding, in vivo depletion of CD4$^+$ T cells by the administration of the OKT4 antibody following transplantation of PBMC prevented the engraftment of EBV-infected T and NK cells. This is the first report of animal models of CAEBV and EBV-HLH that are expected to be useful tools in the development of novel therapeutic strategies for the treatment of the diseases.

Citation: Imadome K-I, Yajima M, Arai A, Nakazawa A, Kawano F, et al. (2011) Novel Mouse Xenograft Models Reveal a Critical Role of CD4$^+$ T Cells in the Proliferation of EBV-Infected T and NK Cells. PLoS Pathog 7(10): e1002326. doi:10.1371/journal.ppat.1002326

Editor: Shou-Jiang Gao, University of Texas Health Science Center San Antonio, United States of America

Received January 27, 2011; **Accepted** September 2, 2011; **Published** October 20, 2011

Funding: This study was supported by grants from the Ministry of Health, Labour and Welfare of Japan (H22-Nanchi-080 and H22-AIDS-002), the Grant of National Center for Child Health and Development (22A-9), a grant for the Research on Publicly Essential Drugs and Medical Devices from The Japan Health Sciences Foundation (KHC1014), and the Grant-in-Aid for Scientific Research (C) (H22-22590374). The funders had no role in study design, data collection and analysis, decision to publish, or preparation of the manuscript.

Competing Interests: The authors have declared that no competing interests exist.

* E-mail: imadome@nch.go.jp (KI); shige@nch.go.jp (SF)

¤ Current address: Department of Microbiology, Yong Loo Lin School of Medicine, National University of Singapore, Singapore

☯ These authors contributed equally to this work.

Introduction

Epstein-Barr virus (EBV) is a ubiquitous γ-herpesvirus that infects more than 90% of the adult population in the world. EBV is occasionally involved in the pathogenesis of malignant tumors, such as Burkitt lymphoma, Hodgkin lymphoma, and nasopharyngeal carcinoma, along with the post-transplantation lymphoproliferative disorders in immunocompromised hosts. Although EBV infection is asymptomatic in most immunologically competent hosts, it sometimes causes infectious mononucleosis (IM), when primarily infecting adolescents and young adults [1]. EBV infects human B cells efficiently in vitro and transform them into lymphoblastoid cell lines (LCLs) [2]. Experimental infection of T and NK cells, in contrast, is practically impossible except in limited conditions [3,4]. Nevertheless, EBV has been consistently demonstrated in T or NK cells proliferating monoclonally or oligoclonally in a group of diseases including chronic active EBV infection (CAEBV) and EBV-associated hemophagocytic lymphohistiocytosis (EBV-HLH) [5,6,7,8,9,10]. CAEBV, largely overlapping the systemic EBV$^+$ T-cell lymphoproliferative diseases of childhood defined in the WHO classification of lymphomas [11], is characterized by prolonged or relapsing IM-like symptoms, unusual patterns of antibody responses to EBV, and elevated EBV DNA load in the peripheral blood [12,13,14]. CAEBV has a chronic time course with generally poor prognosis; without a proper treatment by hematopoietic stem cell transplantation, the

Author Summary

Epstein-Barr virus (EBV) is a ubiquitous human herpesvirus that infects more than 90% of the adult human population in the world. EBV usually infects B lymphocytes and does not produce symptoms in infected individuals, but in rare occasions it infects T or NK lymphocytes and causes severe diseases such as chronic active EBV infection (CAEBV) and EBV-associated hemophagocytic lymphohistiocytosis (EBV-HLH). We developed mouse models of these two human diseases in which EBV-infected T or NK lymphocytes proliferate in mouse tissues and reproduce human pathologic conditions such as overproduction of small proteins called "cytokines" that produce inflammatory responses in the body. These mouse models are thought to be very useful for the elucidation of the pathogenesis of CAEBV and EBV-HLH as well as for the development of therapeutic strategies for the treatment of these diseases. Experiments with the models demonstrated that a subset of lymphocytes called CD4-positive lymphocytes are essential for the proliferation of EBV-infected T and NK cells. This result implies that removal of CD4-positive lymphocytes or suppression of their functions may be an effective strategy for the treatment of CAEBV and EBV-HLH.

majority of cases eventually develop malignant lymphoma of T or NK lineages, multi-organ failure, or other life-threatening conditions. Monoclonal or oligoclonal proliferation of EBV-infected T and NK cells, an essential feature of CAEBV, implies its malignant nature, but other characteristics of CAEBV do not necessarily support this notion. For example, EBV-infected T or NK cells freshly isolated from CAEBV patients, as well as established cell lines derived from them, do not have morphological atypia and do not engraft either in nude mice or *scid* mice (Shimizu, N., unpublished results). Clinically, CAEBV has a chronic time course and patients may live for many years without progression of the disease [15]. Although patients with CAEBV do not show signs of explicit immunodeficiency, some of them present a deficiency in NK-cell activity or in EBV-specific T-cell responses, implying a role for subtle immunodeficiency in its pathogenesis [16,17,18].

EBV-HLH is the most common and the severest type of virus-associated HLH and, similar to CAEBV, characterized by monoclonal or oligoclonal proliferation of EBV-infected T (most often $CD8^+$ T) cells [5,6]. Clinical features of EBV-HLH include high fever, pancytopenia, coagulation abnormalities, hepatosplenomegaly, liver dysfunction, and hemophagocytosis [19]. Overproduction of cytokines by EBV-infected T cells as well as by activated macrophages and T cells reacting to EBV is thought to play a central role in the pathogenesis [20]. Although EBV-HLH is an aggressive disease requiring intensive clinical interventions, it may be cured, in contrast to CAEBV, by proper treatment with immunomodulating drugs [21]. No appropriate animal models have been so far developed for either CAEBV or EBV-HLH.

NOD/Shi-*scid*/IL-2Rγ^{null} (referred here as NOG) is a highly immunodeficient mouse strain totally lacking T, B, and NK lymphocytes, and transplantation of human hematopoietic stem cells to NOG mice results in reconstitution of human immune system components, including T, B, NK cells, dendritic cells, and macrophages [22,23]. These so called humanized mice have been utilized as animal models for the infection of certain human viruses targeting the hemato-immune system, including human immunodeficiency virus 1 (HIV-1) and EBV [24,25,26,27,28,29,30]. Xenotransplantation of human tumor cells to NOG mice also provided model systems for several hematologic malignancies [31,32,33]. To facilitate investigations on the pathogenesis of CAEBV and EBV-HLH and assist the development of novel therapeutic strategies, we generated mouse models of these two EBV-associated diseases by transplanting NOG mice with PBMC isolated from patients with the diseases. In these models, EBV-infected T, NK, or B cells engrafted in NOG mice and reproduced lymphoproliferative disorder similar to either CAEBV or EBV-HLH. Further experiments with the models revealed a critical role of $CD4^+$ T cells in the in vivo proliferation of EBV-infected T and NK cells.

Results

Engraftment of EBV-infected T and NK cells in NOG mice following xenotransplantation with PBMC of CAEBV patients

Depending on the immunophenotypic subset in which EBV causes lymphoproliferation, CAEBV is classified into the T-cell and NK-cell types, with the former being further divided into the CD4, CD8, and γδT types. The nine patients with CAEBV examined in this study are characterized in Table 1 and include all these four types. Intravenous injection of $1-4\times10^6$ PBMC isolated from these nine patients resulted in successful engraftment of EBV-infected T or NK cells in NOG mice in a reproducible manner (Table 1). The results with the patient 1 (CD4 type), patient 3 (CD8 type), patient 5 (γδT type), and patient 9 (NK type) are shown in Figure 1. Seven to nine weeks post-transplantation, EBV DNA was detected in the peripheral blood of recipient mice and reached the levels of 10^5–10^8 copies/μg DNA (Figure 1A). By contrast, no engraftment of EBV-infected cells was observed when immunophenotypic fractions containing EBV DNA were isolated from PBMC and injected to NOG mice (Figure 1A and Table 2). An exception was the $CD4^+$ T-cell fraction isolated from patients with the CD4 type CAEBV, that reproducibly engrafted when transplanted without other components of PBMC (Figure 1A, Table 2). Flow cytometry revealed that the major population of engrafted cells was either $CD4^+$, $CD8^+$, TCRγδor $CD16^+CD56^+$, depending on the type of the donor CAEBV patient (Figure 1B). EBV-infected cells of identical immunophenotypes were found in the patients and the corresponding mice that received their respective PBMC (Figure 1B). Although human cells of multiple immunophenotypes were present in most recipient mice, fractionation by magnetic beads-conjugated antibodies and subsequent real-time PCR analysis detected EBV DNA only in the predominant immunophenotypes that contained EBV DNA in the original patients (Figure 1B, Table 1). The EBV DNA load observed in individual lymphocyte subsets in the patient 3 and a mouse that received her PBMC is shown as supporting data (Table S1). When PBMC from three healthy EBV-carriers were injected intravenously to NOG mice, as controls, no EBV DNA was detected from either the peripheral blood, spleen, or liver (data not shown). Histological analyses of the spleen and the liver of these control mice identified no EBV-encoded small RNA (EBER)-positive cells, although some CD3-positive human T cells were observed (Figure S2). Analysis of TCR Vβ repertoire demonstrated an identical predominant T-cell clone in patients (patients 1 and 3) and the corresponding mice that received their PBMC (Figure 1C). The general condition of most recipient mice deteriorated gradually in the observation period of eight to twelve weeks, with loss of body weight (Figure S1), ruffled hair, and inactivity.

NOG mice engrafted with EBV-infected T or NK cells were sacrificed for pathological and virological analyses between eight

Table 1. Patients with EBV-T/NK LPD and the results of xenotransplantation of their PBMC to NOG mice.

Patient number	Diagnosis	Sex	Age	Type of infected cells	[1]EBV DNA load in the patients	[2]Engrafted cells in mice	[3]Engraftment	[1]EBV DNA load in mice
1	CAEBV	F	25	CD4	9.2×10^5	CD4, CD8	3/3	$1.0\sim3.8\times10^7$
2	CAEBV	M	46	CD4	$1.3\sim7.2\times10^5$	CD4, CD8	2/2, 3/3	$2.6\sim10\times10^5$
3	CAEBV	F	35	CD8	$2.1\sim78\times10^5$	CD8, CD4	2/2, 2/2	$1.1\sim33\times10^6$
4	CAEBV	M	28	CD8	8.2×10^5	CD8, CD4	3/3	$1.1\sim2.5\times10^6$
5	CAEBV	M	10	γδT	2.2×10^6	γδT, CD4, CD8	2/2	$3.8\sim6.5\times10^6$
6	CAEBV	F	15	γδT	6.2×10^5	γδT, CD4, CD8	2/2	$2.2\sim11\times10^5$
7	CAEBV	M	13	NK	$1.1\sim6.7\times10^5$	NK, CD4, CD8	2/2, 2/2	$0.6\sim15\times10^4$
8	CAEBV	F	13	NK	6.3×10^6	NK, CD4, CD8	3/3, 2/2	$0.8\sim1.9\times10^5$
9	CAEBV	M	8	NK	$1.2\sim8.7\times10^5$	NK, CD4, CD8	2/2, 3/3	$1.8\sim7.2\times10^5$
10	EBV-HLH	M	10	CD8	$2.8\sim38\times10^4$	CD8, CD4	2/2, 2/2	$6.5\sim9.9\times10^4$
11	EBV-HLH	M	50	CD8	6.2×10^5	CD8, CD4	4/4	$7.0\sim45\times10^4$
12	EBV-HLH	M	1	CD8	3.1×10^5	CD8, CD4	2/2	$6.0\sim9.1\times10^4$
13	EBV-HLH	M	64	CD8	$3.2\sim3.9\times10^5$	CD8, CD4	2/2, 2/2	$5.0\sim30\times10^5$

[1]EBV DNA copies/μg DNA in the peripheral blood.
[2]EBV DNA was detected only in the cells of the underlined subsets.
[3]Number of mice with successful engraftment per number of recipient mice is shown for each experiment.
doi:10.1371/journal.ppat.1002326.t001

and twelve weeks post-transplantation. On autopsy, the majority of mice presented with splenomegaly, with slight hepatomegaly in occasional cases (Figure 2A). Histopathological findings obtained from a representative mouse (recipient of PBMC from the patient 3 (CD8 type)) are shown in Figure 2B and reveal infiltration of human $CD3^+CD20^-$ cells to major organs, including the spleen, liver, lungs, kidneys, and small intestine. These cells were positive for both EBER and human CD45RO, indicating that they are EBV-infected human T cells (Figure 2B). In contrast, no EBV-infected T cells were found in mice transplanted with PBMC isolated from a normal EBV carrier (Figure S2). Histopathology of a control NOG mouse is shown in Figure S2. Morphologically, EBV-infected cells are relatively small and do not have marked atypia. The infiltration pattern was leukemic and identical with chronic active EBV infection in children [34]. The architecture of the organs was well preserved in spite of marked lymphoid infiltration. The spleen showed marked expansion of periarterial lymphatic sheath owing to lymphocytic infiltration. In the liver, a dense lymphocytic infiltration was observed in the portal area and in the sinusoid. The lung showed a picture of interstitial pneumonitis and the lymphocytes often formed nodular aggregations around bronchioles and arteries. In the kidney, dense lymphocytic infiltration caused interstitial nephritis. In the small intestine, mild lymphoid infiltration was seen in mucosa. Quantification of EBV DNA in the spleen, liver, lymph nodes, lungs, kidneys, adrenals, and small intestine of this mouse revealed EBV DNA at the levels of $1.5\text{–}5.1\times10^7$ copies/μg DNA. Mice transplanted with PBMC derived from CAEBV of other types exhibited similar infiltration of EBV-infected T or NK cells to the spleen, liver, and other organs (Figure 2C and data not shown).

EBV-infected T- and NK-cell lines established from CAEBV patients do not engraft in NOG mice

We established EBV-positive cell lines of $CD4^+$ T, $CD8^+$ T, γδT, and $CD56^+$ NK lineages from PBMC of the patients listed in Table 1 by the method described previously [35], and confirmed by flow cytometry that the surface phenotypes of EBV-infected cells in the original patients were retained in these cell lines (data not shown). To test whether these cell lines engraft in NOG mice, $1\text{–}4\times10^6$ cells were injected intravenously to NOG mice. The results are shown in Figure 3A and indicate that CAEBV-derived cell lines of the $CD8^+$ T, γδT, and $CD56^+$ NK phenotypes do not engraft in NOG mice. Neither human CD45-positive cells nor EBV DNA were detected in the peripheral blood of the mice up to twelve weeks post-transplantation. When the recipient mice were sacrificed at twelve weeks post-injection, no EBV DNA could be detected in the spleen, liver, bone marrow, mesenteric lymph nodes, and kidneys. In contrast, the $CD4^+$ T cell lines derived from the CD4-type patients 1 and 2 engrafted in NOG mice and induced T lymphoproliferation similar to that induced by PBMC isolated freshly from these patients (Figure 3A and data not shown). These results, together with the results of transplantation with EBV-containing subsets of PBMC, indicate that EBV-infected T and NK cells, with the exception of those of the $CD4^+$ subset, are not able to engraft in NOG mice, when they are separated from other components of PBMC, suggesting that some components of PBMC are essential for the outgrowth EBV-infected T and NK cells in NOG mice.

Engraftment of EBV-infected T and NK cells in NOG mice requires $CD4^+$ T cells

To identify the cellular component required for the engraftment of EBV-infected T and NK cells in NOG mice, we transplanted PBMC of CAEBV patients after removing individual immunophenotypic subsets by magnetic beads-conjugated antibodies. The results are shown in Figure 3B and summarized in Table 2. With respect to the patients 3 and 4, in whom $CD8^+$ T cells are infected with EBV, removal of $CD8^+$ cells from PBMC, as expected, resulted in the failure of engraftment, whereas elimination of $CD19^+$, $CD56^+$, or $CD14^+$ cells did not affect engraftment. Importantly, elimination of $CD4^+$ cell fraction, that did not contain EBV DNA, resulted in the failure of engraftment of EBV-infected T cells (Figure 3B and data not shown). In the experiments with the patients 5 and 6, in whom γδT cells were infected, removal $CD4^+$ cells that did not contain EBV DNA, as well as that of γδT cells, resulted in the failure of engraftment.

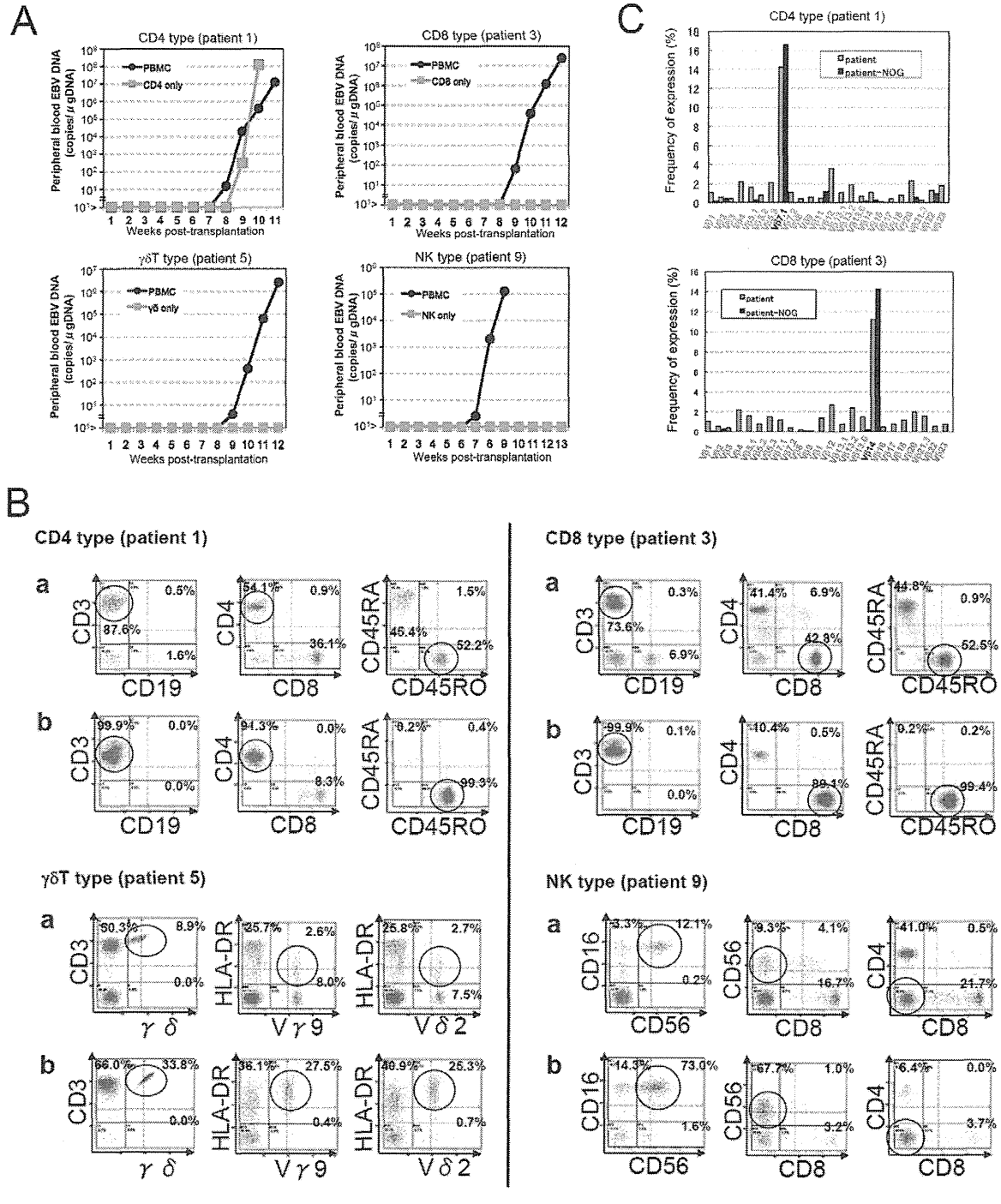

Figure 1. Engraftment of EBV-infected T or NK cells in NOG mice following transplantation with PBMC of patients with CAEBV. A. Measurement of EBV DNA levels. PBMC obtained from the CAEBV patients 1 (CD4 type), 3 (CD8 type), 5 (γδT type), and 9 (NK type) were injected intravenously to NOG mice and EBV DNA load in their peripheral blood was measured weekly by real-time PCR. The results of transplantation with whole PBMC or with isolated EBV DNA-containing cell fraction are shown. B. Flow-cytometric analysis on the expression of surface markers in the peripheral blood lymphocytes of patients (a) with CAEBV and NOG mice (b) that received PBMC from them. Human lymphocytes gated by the pattern of side scatter and human CD45 expression were further analyzed for the expression of various surface markers indicated in the figures. The results from the patients 1, 3, 5, and 9, and the corresponding mice that received their respective PBMC are shown. Circles indicate the fractions that contained EBV DNA. C. Analysis on the expression of TCR Vβ repertoire. Peripheral blood lymphocytes obtained from the patients 1 (CD4 type) and 3 (CD8 type), and from the corresponding mice that received their respective PBMC were analyzed for the expression of Vβ alleles. The percentages of T cells expressing each Vβ allele are shown for the patients (grey bars) and the mice (black bars).
doi:10.1371/journal.ppat.1002326.g001

Removal of $CD8^+$, $CD14^+$, $CD19^+$, or $CD56^+$ cells did not have an influence on the engraftment (Figure 3B and data not shown). Regarding the patients 8 an 9 in whom EBV resided in $CD56^+$ NK cells, removal of $CD4^+$ as well as $CD56^+$ cells resulted in the failure of engraftment, whereas that of $CD8^+$, $CD19^+$, or $CD14^+$ cells did not affect engraftment (Figure 3B and data not shown). In

Table 2. Results of xenotransplantation with subsets of PBMC obtained from CAEBV patients.

Number of patient	Diagnosis	Phenotype of infected cells	Cell fraction transplanted	Number of transplanted cells	Engraftment
1	CAEBV	CD4	PBMC	2×10^6	+
			CD4	2×10^6	+
			PBMC-CD4	3×10^6	–
			PBMC-CD8	2×10^6	+
			PBMC-CD56	2×10^6	+
			PBMC-CD14	2×10^6	+
			PBMC-CD19	2×10^6	+
3	CAEBV	CD8	PBMC	2×10^6	+
			CD8	3×10^6	–
			PBMC-CD4	3×10^6	–
			PBMC-CD8	3×10^6	–
			PBMC-CD56	2×10^6	+
			PBMC-CD14	2×10^6	+
			PBMC-CD19	2×10^6	+
5	CAEBV	γδT	PBMC	2×10^6	+
			γδT	3×10^6	–
			PBMC-CD4	3×10^6	–
			PBMC-γδT	3×10^6	–
			PBMC- CD8	3×10^6	+
			PBMC-CD56	3×10^6	+
			PBMC-CD14	3×10^6	+
			PBMC-CD19	3×10^6	+
9	CAEBV	NK	PBMC	2×10^6	+
			NK	3×10^6	–
			PBMC-CD4	3×10^6	–
			PBMC-CD8	3×10^6	+
			PBMC-CD56	3×10^6	–
			PBMC-CD14	3×10^6	+
			PBMC-CD19	3×10^6	+
11	EBV-HLH	CD8	PBMC	2×10^6	+
			PBMC-CD4	4×10^6	–

doi:10.1371/journal.ppat.1002326.t002

the patients 1 and 2, in whom $CD4^+$ T cells were infected, only the removal of $CD4^+$ cells blocked the engraftment of EBV-infected cells and depletion of either $CD8^+$, $CD19^+$, or $CD14^+$ cells had no effect (Figure 3B and data not shown). These results suggested that EBV-infected cells of the $CD8^+$, γδT, and $CD56^+$ lineages require $CD4^+$ cells for their engraftment in NOG mice. To confirm this interpretation, we performed complementation experiments, in which EBV-containing fractions of the $CD8^+$ (patient 4), γδT (patient 5), or $CD56^+$ (patient 7) phenotypes were transplanted together with autologous $CD4^+$ cells. The results are shown in Figure 3A and indicate that EBV-infected $CD8^+$, γδT, or $CD56^+$ cells engraft in NOG mice when transplanted together with $CD4^+$ cells. Similarly, when EBV-infected cell lines of the $CD8^+$, γδT, and $CD16^+$ lineages were injected intravenously to NOG mice together with autologous $CD4^+$ cells, these cell lines engrafted to the mice (Figure 3A). Finally, to further confirm the essential role of $CD4^+$ cells, we examined the effect of the OKT-4 antibody that depletes $CD4^+$ cells in vivo [24]. PBMC isolated from the CAEBV patient 3 (CD8 type) and the patient 8 (NK type) were injected intravenously to NOG mice and OKT-4 was administered intravenously for four consecutive days starting from the day of transplantation. The results are shown in Figure 4 and indicate that OKT-4 can strongly suppress the engraftment of EBV-infected T and NK cells. In the mice treated with OKT-4, no splenomegaly was observed and EBV DNA was not detected either in the peripheral blood, spleen, liver, or lungs at eight weeks post-transplantation.

Analysis on the EBV gene expression associated with T or NK lymphoproliferation in NOG mice

Previous analysis of EBV gene expression in patients with CAEBV revealed the expression of EBNA1, LMP1, and LMP2A with the involvement of the Q promoter in the EBNA genes transcription and no expression of EBNA2, being consistent with the latency II type of EBV gene expression [36,37,38]. To test whether EBV-infected T and NK cells that proliferate in NOG mice retain this type of viral gene expression, we performed RT-PCR analysis in the spleen and the liver of mice that received

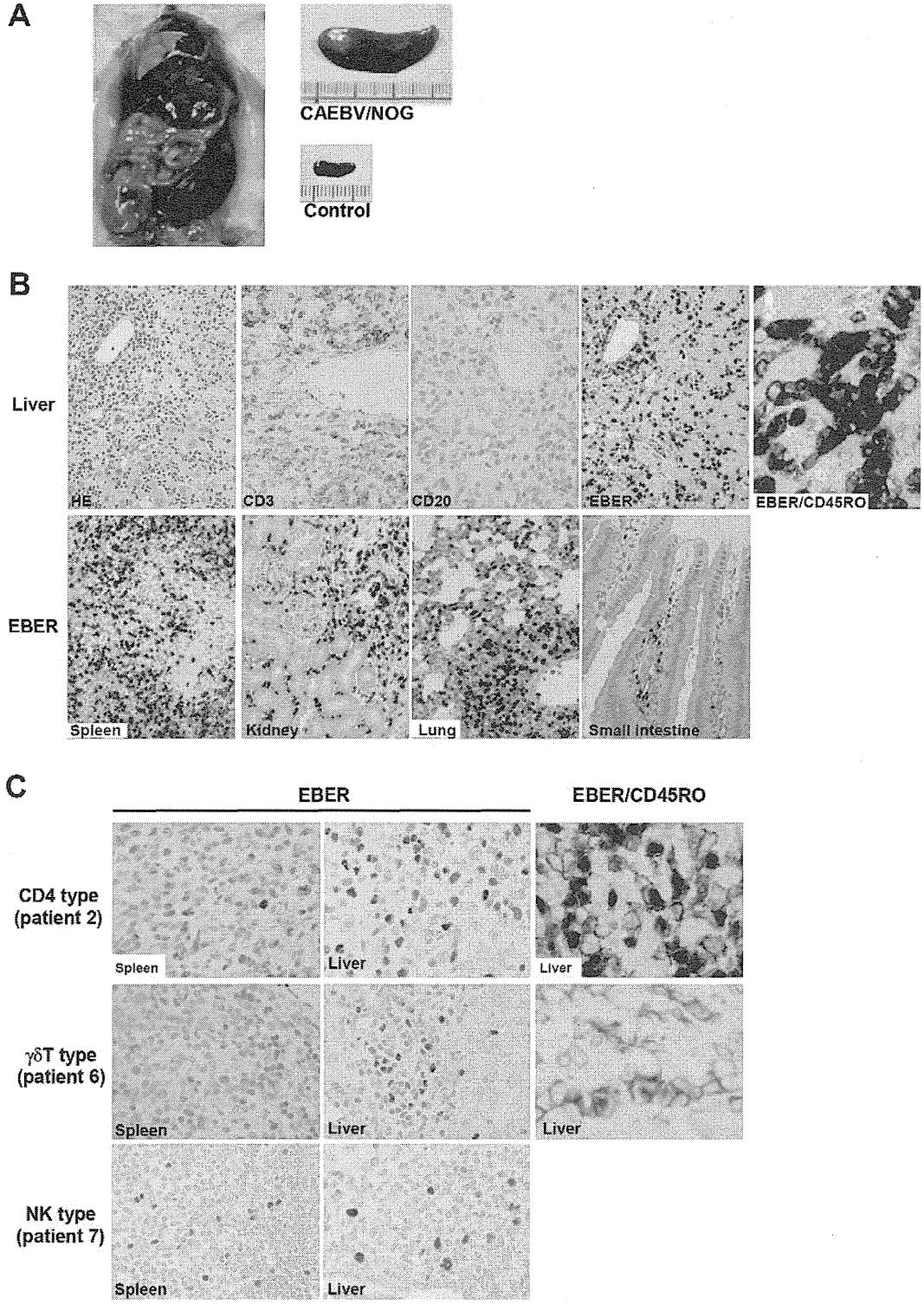

Figure 2. Pathological and immunochemical analyses on NOG mice transplanted with PBMC from CAEBV patients. A. Photographs of a model mouse showing splenomegaly and of the excised spleen. This mouse was transplanted with PBMC from the CAEBV patient 3 (CD8 type). Spleen from a control NOG mouse is also shown. B. Photomicrographs of various tissues of a mouse that received PBMC from the patient 3 (CD8 type). Upper panels: liver tissue was stained with hematoxylin-eosin (HE), antibodies specific to human CD3 or CD20, or by ISH with an EBER probe; the rightmost panel is a double staining with EBER and human CD45RO. Bottom panels: EBER ISH in the spleen, kidney, lung, and small intestine. Original magnification is ×200, except for EBER/CD45RO, that is ×400. C. Photomicrographs of the spleen and liver tissues obtained from NOG mice transplanted with PBMC from the CAEBV patients 2 (CD4 type), 6 (γδT type) or 7 (NK type). Tissues were stained by EBER-ISH or by double staining with EBER-ISH and human CD45RO. Original magnification ×600.
doi:10.1371/journal.ppat.1002326.g002

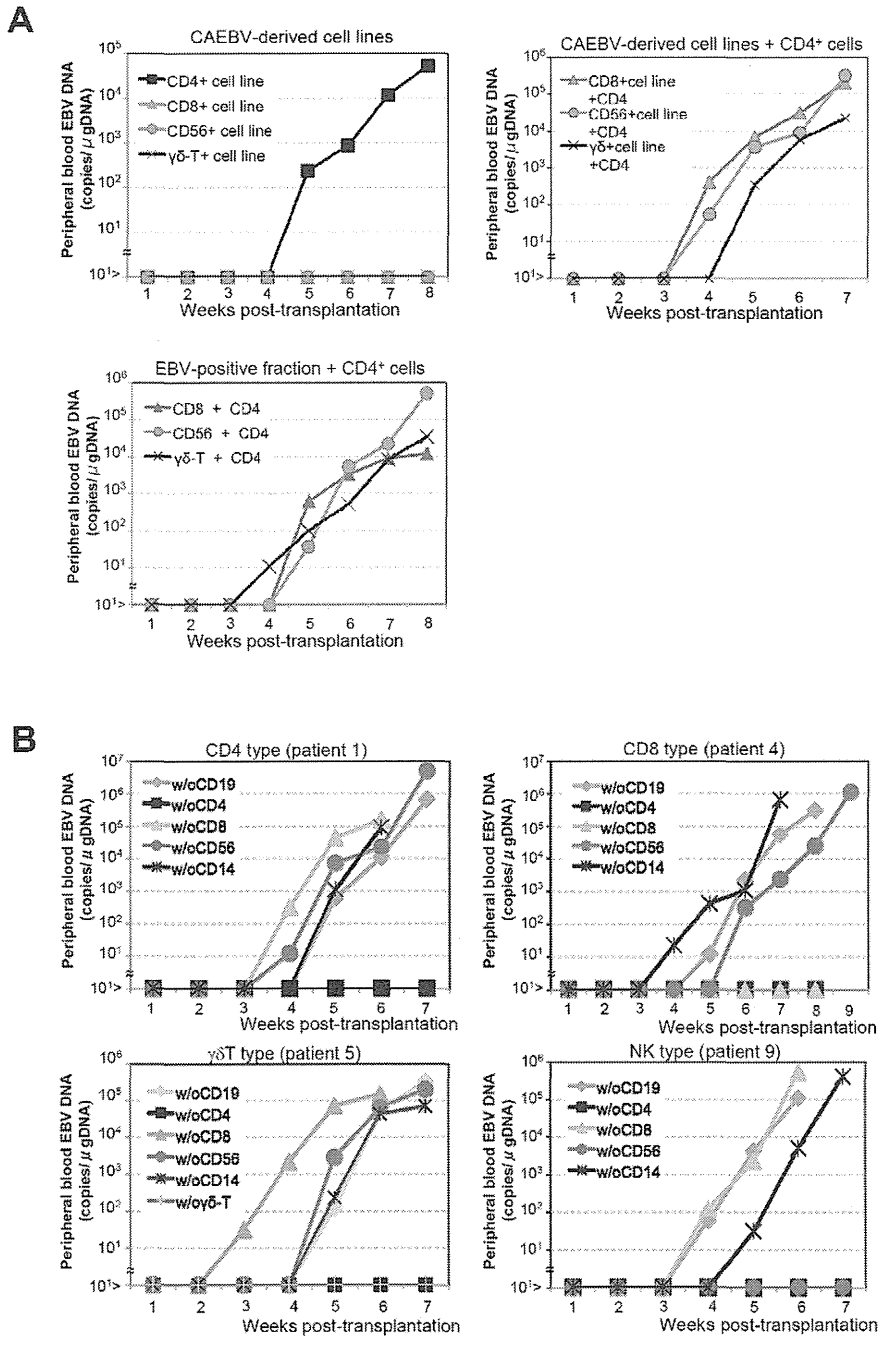

Figure 3. Analysis on the conditions of the engraftment of EBV-infected T and NK cells in NOG mice. A. EBV-infected T or NK cells isolated from patients with CAEBV or cell lines derived from them were injected to NOG mice in the conditions described below. Peripheral blood EBV DNA levels were then measured weekly. Upper-left panel: 5×10^6 cells of EBV-infected $CD4^+$ T, $CD8^+$ T, γδT, and $CD56^+$ NK cell lines established from the CAEBV patients 1, 4, 6, and 8, respectively, were injected intravenously to NOG mice. Upper-right panel: 5×10^6 cells of the $CD8^+$ T, γδT, and $CD56^+$ NK cell lines established from the patients 3, 6, and 8, respectively, were injected intravenously to NOG mice together with autologous $CD4^+$ T cells isolated from 5×10^6 PBMC. Bottom panel: 5×10^6 cells of the $CD8^+$ T, γδT, and $CD56^+$ NK fractions isolated freshly from the patients 4, 5, and 7, respectively, were injected intravenously to NOG mice together with autologous $CD4^+$ T cells isolated from 5×10^6 PBMC. B. Transplantation of PBMC devoid of individual immunophenotypic subsets to NOG mice. $CD19^+$, $CD4^+$, $CD8^+$, $CD56^+$, or $CD14^+$ cells were removed from PBMC obtained from the patient 1 (CD4 type, upper-left panel), 4 (CD8 type, upper-right), 5 (γδT type, bottom-left), and 9 (NK type, bottom-right) and the remaining cells were injected intravenously to NOG mice. Thereafter peripheral blood EBV DNA was determined weekly.
doi:10.1371/journal.ppat.1002326.g003

PBMC from the CAEBV patient 3 (CD8 type). The results are shown in Figure 5A and demonstrate the expression of mRNAs coding for EBNA1, LMP1, LMP2A, and LMP2B, but not for EBNA2. Expression of the EBV-encoded small RNA 1 (EBER1) was also demonstrated. EBNA1 mRNAs transcribed from either the Cp promoter or the Wp promoter were not detected, whereas those transcribed from the Q promoter was abundantly detected. These results indicate that EBV-infected T cells retain the latency

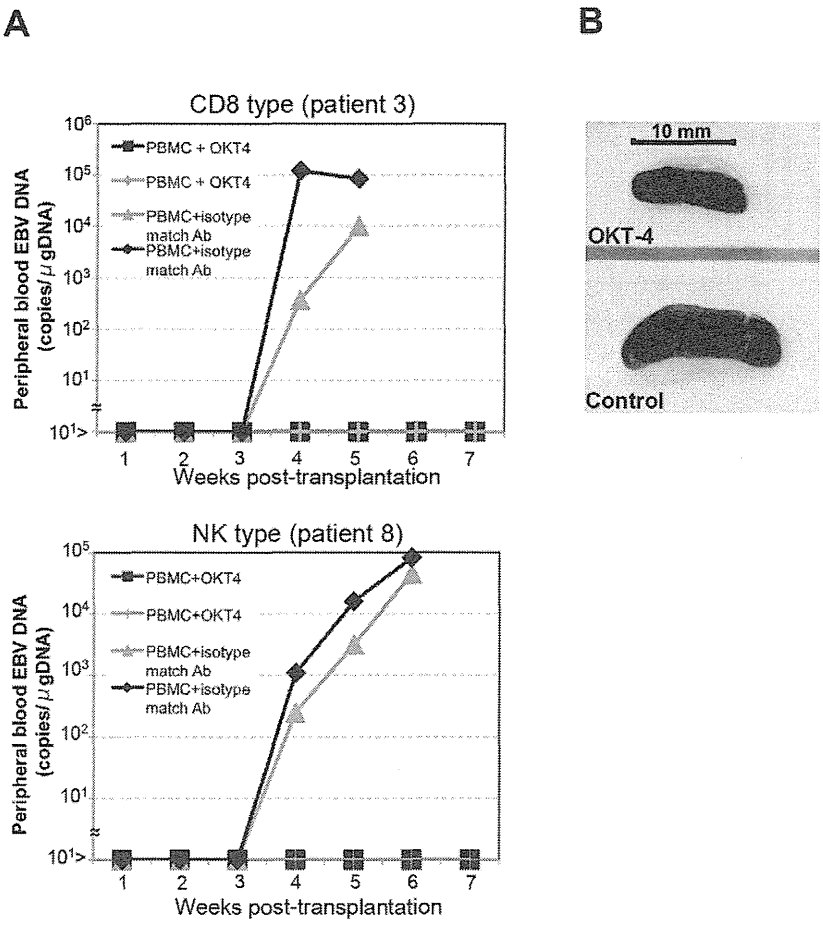

Figure 4. Suppression of the engraftment of EBV-infected T and NK cells by the OKT-4 antibody. PBMC (5×10^6 cells) isolated from the CAEBV patient 3 (CD8 type) or 8 (NK type) were injected intravenously to NOG mice. The OKT-4 antibody (100 μg/mouse) was administered intravenously on the same day of transplantation and the following three consecutive days. As a control, isotype-matched mouse IgG was injected. A. Changes in the peripheral blood EBV DNA level in the recipient mice. Results with the mice transplanted with PBMC of the patient 3 (top) and of the patient 8 (bottom) are shown. B. Photographs of the spleen of an OKT-4-treated mouse (top) and a control mouse (bottom) taken at autopsy.
doi:10.1371/journal.ppat.1002326.g004

II pattern of latent EBV gene expression after engraftment in NOG mice. Similar analyses with NOG mice engrafted with EBV-infected NK cells also showed the latency II type of EBV gene expression (data not shown).

NOG mice engrafted with EBV-infected T or NK cells produce high levels of human cytokines

In patients with CAEBV, high levels of cytokines have been detected in the peripheral blood and are thought to play important roles in the pathogenesis [20,39,40]. To test whether this hypercytokinemia is reproduced in NOG mice, we examined the levels of various human cytokines in the sera of transplanted mice using ELISA kits that can quantify human cytokines specifically. The results are shown in Figure 5B and indicate that the mice transplanted with PBMC of the patient 3 (CD8 type) or the patient 8 (NK type) contained high levels of RANTES, IFN-γ, and IL-8 in their sera.

Engraftment of EBV-infected T and B cells derived from patients with EBV-HLH in NOG mice

To extend the findings obtained from the CAEBV xenograft model to another disease with EBV^+ T/NK lymphoproliferation, we transplanted NOG mice with PBMC isolated from patients with EBV-HLH. Characteristics of the four EBV-HLH patients examined in this study and the results of transplantation with their PBMC are summarized in Table 1. EBV DNA was detected in the peripheral blood three to four weeks post-transplantation and rapidly reached the levels of 1×10^4 to 1×10^6 copies/μg DNA (results of typical experiments are shown in Figure 6A). Similar to the findings in CAEBV, EBV DNA was not detected in the recipient mice, when $CD4^+$ cell fraction was removed from PBMC (Figure 6A). Immunophenotypic analyses on the peripheral blood lymphocytes isolated from EBV-HLH patients and corresponding recipient mice revealed that cells of an identical immunophenotype ($CD3^+CD8^+CD45RO^+CD19^-CD4^-CD45RA^-CD16^-CD56^-$) were present and contained EBV DNA in both the patients and corresponding mice (Figure 6C and data not shown). The EBV DNA load observed in individual lymphocyte subsets in the patient 10 and a mouse that received his PBMC is shown as supporting data (Table S2). General condition of the recipient mice deteriorated consistently more quickly, with the loss of body weight (Figure S1), ruffling of hair, and general inactivity, than those mice engrafted with EBV-infected T or NK cells derived from CAEBV. The mice were sacrificed around four weeks post-transplantation for pathological analyses. Macroscopical observation revealed moderate to severe splenomegaly (Figure 6D) in the

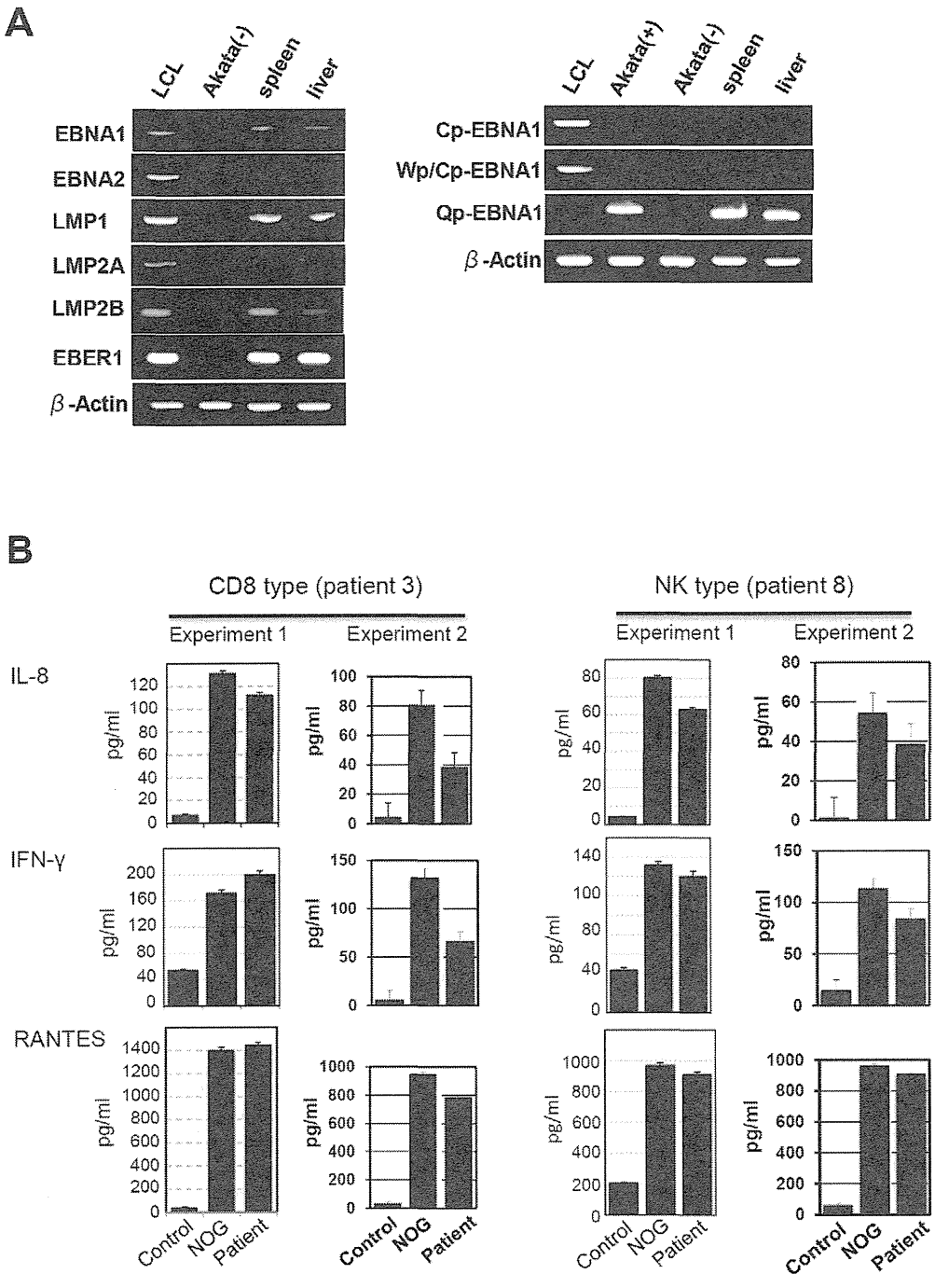

Figure 5. Analyses on the latent EBV gene expression and cytokine production in NOG mice transplanted with PBMC of CAEBV patients. A. EBV gene expression. Total RNA was purified from the spleen and liver of a mouse that received PBMC from the patient 3 (CD8 type) and applied for RT-PCR assay to detect transcripts from the indicated genes. RNA samples from an EBV-transformed B-lymphoblastoid cell line (LCL) and from EBV-negative Akata cell line were used as positive and negative controls, respectively. The primers used in the experiments are shown in Materials and Methods. B. Quantification of plasma levels of human cytokines in patients with CAEBV and corresponding recipient mice. PBMC were isolated from the patients 3 (CD8 type) and 8 (NK type) in two occasions and transplanted to NOG mice. Plasma cytokine levels of the patients were determined when their PBMC were isolated. Plasma cytokine levels of the corresponding recipient mice, prepared on each occasion of PBMC collection, were determined when they were sacrificed. Concentration of human IL-8, IFN-γ, and RANTES were measured by appropriate ELISA kits following the instruction provided by the manufacturer. Plasma samples from healthy adults were used as a control. The bars represent mean values and standard errors from triplicate measurements.
doi:10.1371/journal.ppat.1002326.g005

majority of recipient mice, and slight hepatomegaly in a limited fraction of them. A finding characteristic to these mice were massive hemorrhages in the abdominal and/or thoracic cavities, that were not seen in the mice transplanted with CAEBV-derived PBMC (Figure 6D and data not shown). These hemorrhagic lesions may reflect coagulation abnormalities characteristic to

HLH. Histopathological analyses revealed a number of $EBER^+$ cells in the spleen and the liver (Figure 6E) and quantification of EBV DNA in these tissues revealed 1.4×10^1 to 2.4×10^2 copies/μg of EBV DNA. When the tissues were examined by immunostaining and EBER ISH, the $EBER^+$ cells were shown unexpectedly to be mostly $CD45RO^-$ and $CD20^+$ in all five transplantation experiments with four different patients, indicating that the majority of EBV-infected cells in these tissues are of the B-cell lineage (Figure 6E and data not shown). $EBER^+$ large B cells were seen scattered among numerous reactive small T cells, most of which are $CD8^+$, in the tissues of the spleen, liver, lungs and kidneys. A number of macrophages were also seen in these tissues. Fractionation of mononuclear cells obtained from the liver of a mouse transplanted with PBMC of the EBV-HLH patient 10, followed by real-time PCR, detected EBV DNA (1.4×10^1 copies/μg DNA) only in the $CD19^+$ B-cell fraction. In addition, an EBV-infected B lymphoblastoid cell line, but not an EBV-positive T cell line, could be established from this liver. Thus the presence of EBV in B cells were demonstrated by three independent methods in the tissues of EBV-HLH mice. Enzyme-linked immunosorbent assay revealed extremely high levels of human cytokines, including IL-8, IFN-γ, and RANTES, in the sera of both the original patients and the recipient mice (Figure 6B). The levels of IL-8 and IFN-γ were much higher than those observed in the peripheral blood of patients with CAEBV and mice that received their PBMC. Thus, NOG mice transplanted with EBV-HLH-derived PBMC are distinct from those transplanted with CAEBV-derived PBMC in the aggressive time course of the disease, internal hemorrhagic lesions, extremely high levels of IL-8 and IFN-γ in the peripheral blood, and the presence of EBV-infected B cells in lymphoid tissues.

Discussion

The mouse xenograft models of CAEBV and EBV-HLH developed here represent the first recapitulation of EBV-associated T/NK lymphoproliferation in experimental animals. Previously, Hayashi and others inoculated rabbits with Herpesvirus papio and succeeded in the generation of T-cell lymphoproliferative disorder with pathological findings suggestive of EBV-HLH [41]. This model, however, is based on an EBV-related virus and not EBV itself, and therefore may contain features irrelevant to the original human disease. Although the CAEBV and EBV-HLH models described here exhibited some common features, including the abundant presence of EBV-infected T or NK cells in the peripheral blood, there were some critical differences between the two models, probably reflecting the divergence of the pathophysiology of the original diseases. First of all, in the EBV-HLH model mouse, EBV was detected mainly in B cells in the spleen and the liver, while it was found mainly in T cells in the peripheral blood. This makes an obvious contrast with the CAEBV model mouse, where EBV was detected in T or NK cells in both the peripheral blood and lymphoid tissues. We do not have an explanation for the apparent discrepancy in the host cell type of EBV infection between the peripheral blood and lymphoid tissues of the EBV-HLH model. It should be, however, noted that histopathology of EBV-HLH tissues has not been fully investigated and therefore it is still possible that significant number of EBV-infected B cells are present in the lymphoid tissues of EBV-HLH patients. Other differences between the two models include much higher plasma levels of IL-8 and IFN-γ more aggressive and fatal outcome, and internal hemorrhagic lesions in EBV-HLH model mice, probably reflecting the differences in the pathophysiology of the original diseases.

EBV-positive B-cell proliferation was not seen in CAEBV model mice even in long-term observation beyond twelve weeks. This seems puzzling since low but significant amount of EBV DNA was found also in $B19^+$ B-cell fraction in most patients with CAEBV. It should be noted that EBV-infected T or NK cell lines could be established relatively easily from patients with CAEBV by adding recombinant IL-2 in the medium. In contrast, establishment of EBV-infected B LCLs from these patients has been extremely difficult. In fact, we could establish B-LCLs from a few patients with CAEBV only when their PBMC were cultured on feeder cells expressing CD40 ligand. Therefore, we speculate that in the particular context of CAEBV, both in the patient and the model mouse, proliferation of EBV-infected B cells are somehow inhibited by an unknown mechanism.

Analysis on the conditions of engraftment of EBV-infected T/NK cells using these new xenograft models revealed that EBV-infected T and NK cells of the $CD8^+$ T, TCRγδT and $CD56^+$ NK lineages and cell lines derived from them require $CD4^+$ T cells for their engraftment in NOG mice. Only those EBV-infected cells and cell lines of the $CD4^+$ T lineage could engraft in NOG mice on their own. These findings suggest that some factor(s) provided by $CD4^+$ cells are essential for engraftment. Soluble factors produced by $CD4^+$ T cells may be responsible for this function and we are currently examining cytokines, including IL-2, for their ability to support the engraftment of EBV-infected T and NK cells. It is also possible that cell to cell contact involving $CD4^+$ cells is critical for engraftment. This dependence on $CD4^+$ cells represents an interesting consistency with the previous finding that engraftment of EBV-transformed B lymphoblastoid cells in *scid* mice required the presence of $CD4^+$ cells [42,43]. It has been speculated that T cells activated by an EBV-induced superantigen may be involved in the engraftment of EBV-infected B lymphoblastoid cells in *scid* mice [44]. Although a similar superantigen-mediated mechanism might also be assumed in T- and NK-cell lymphoproliferation in NOG mice, the data of TCR repertoire analyses (Figure 1C and data not shown) show no indication for clonal expansion of Vβ13 T cells that are known to be specifically activated by the EBV-induced superantigen HERV-K18. It seems therefore unlikely that this superantigen is involved in the $CD4^+$ T cell-dependent engraftment of EBV-infected T and NK cells. We expect $CD4^+$ T cells and/or molecules produced by them may be an excellent target in novel therapeutic strategies for the treatment of CAEBV and EBV-HLH. In fact, administration of the OKT-4 antibody that depletes $CD4^+$ cells in vivo efficiently prevented the engraftment of EBV-infected T cells. As a next step, we plan to test the effect of post-engraftment administration of OKT-4.

The dependence of EBV-infected T and NK cells on $CD4^+$ T cells for their engraftment in NOG mice suggests the possibility that these cells are not capable of autonomous proliferation. Consistent with this notion, EBV-infected T and NK cell lines, including that of the $CD4^+$ lineage, are dependent on IL-2 for their in vitro growth and do not engraft in either nude mice or *scid* mice when transplanted either s.c. or i.v (Shimizu, N., unpublished results). Clinically, CAEBV is a disease of chronic time course and patients carrying monoclonal EBV-infected T or NK cell population may live for many years without progression of the disease [15]. Overt malignant T or NK lymphoma usually develops only after a long course of the disease. Taking all these findings in consideration, we suppose that EBV-infected cells are not truly malignant at least in the early phase of the disease, even when they appear monoclonal. Because infection of EBV in T or NK cells is not unique to CAEBV and has been recognized also in infectious mononucleosis [45,46], the critical deficiency in

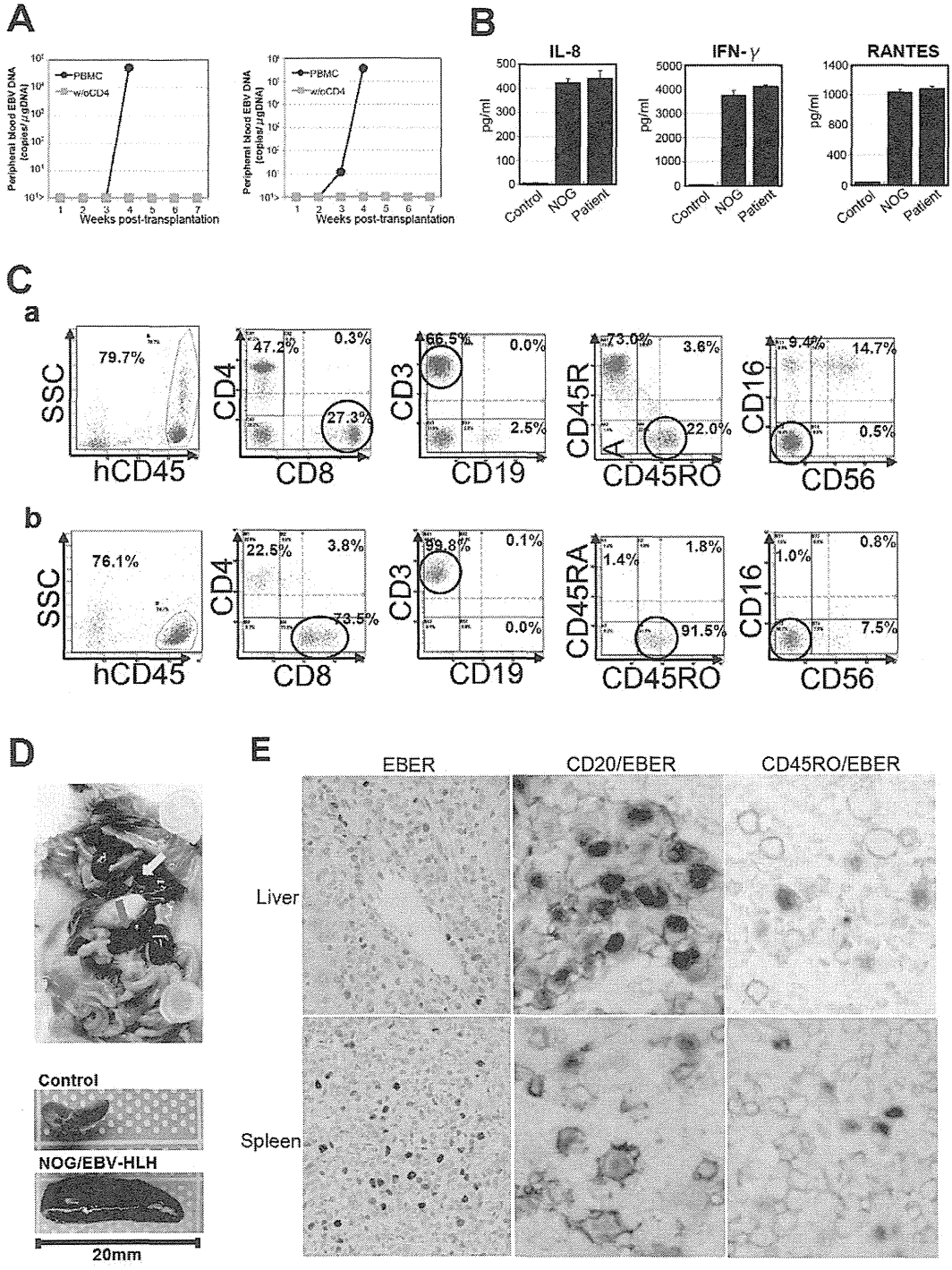

Figure 6. Engraftment of EBV-infected T and B cells in NOG mice transplanted with PBMC of patients with EBV-HLH. A. Peripheral blood EBV DNA load. Following transplantation with PBMC or PBMC devoid of $CD4^+$ cells of the patient 11, EBV DNA was measured weekly by real-time PCR. Results of two mice prepared in an experiment are shown. B. Cytokine levels in the peripheral blood of the patient 12 and a mouse that received his PBMC. The levels of IL-8, IFN-γ, and RANTES were measured by ELISA in triplicates and the means and the standard errors are shown. A plasma sample of healthy person was used as a control. C. Immunophenotypic analyses on the peripheral blood lymphocytes of the EBV-HLH patient 10 (a) and a mouse that received his PBMC (b). Lymphocytes were gated by the pattern of the side scatter and the expression of human CD45, and analyzed for the expression of the indicated markers. The circles indicate the fractions that contained EBV DNA. D. Photograph of a mouse showing splenomegaly (red arrow) and hemorrhagic lesions (yellow arrow). Spleens excised from this mouse and a control mouse are shown at the bottom. E. Photomicrographs of the tissues of mice transplanted with EBV-HLH-derived PBMC. Liver and spleen tissues of a mouse transplanted with PBMC of the patient 11 were examined by EBER-ISH (left), double staining with an anti-human CD20 monoclonal antibody and EBER-ISH (middle), and double staining with an anti-human CD45RO monoclonal antibody and EBER-ISH (right). Original magnification ×600.
doi:10.1371/journal.ppat.1002326.g006

CAEBV may be its inability to immunologically remove EBV-infected T and NK cells. In this context, it should be emphasized that EBV-infected T or NK cells usually exhibit the latency II pattern of EBV gene expression and do not express EBNA3s, that possess immuno-dominant epitopes recognized by EBV-specific T cells [47]. EBV-infected T and NK cells are thus not likely to be removed by cytotoxic T cells as efficiently as EBV-infected B cells that express EBNA3s. The reported lack of cytotoxic T cells specific to LMP2A [17], one of the few immuno-dominant EBV proteins expressed in the virus-infected T and NK cells, may therefore seriously affect the host's capacity to control their proliferation. A genetic defect in the perforin gene was recently identified in a patient with clinical and pathological features resembling CAEBV, suggesting that defects in genes involved in immune responses can result in clinical conditions similar to CAEBV [48].

Engraftment of EBV-infected T and NK cells in NOG mice was in most cases accompanied by co-engraftment of un-infected cell populations. These un-infected cells might have been maintained and induced to proliferate by certain factors produced by EBV-infected T or NK cells. Abundant cytokines produced by these cells may be responsible for this activity. It is also possible that the proliferation of these un-infected cells represents immune responses. Experiments are underway to test whether these un-infected T cells contain EBV-specific cells. These un-infected T cells might also be reacting to host murine tissues. Intravenous injection of PBMC obtained from normal humans to immunodeficient mice including NOG mice has been shown to induce acute or chronic graft versus host disease (GVHD) [49,50]. However, because much less PBMC were injected to mice in the present study as compared to those previous studies, it is not likely that major GVHD was induced in NOG mice transplanted with PBMC of patients with CAEBV or EBV-HLH.

CAEBV has been treated by a variety of regimens, including antiviral, cytocidal, and immunomodulating agents with more or less unsatisfactory results. Although hematopoietic stem cell transplantation, especially that with reduced intensity conditioning can give complete remission in a substantial number of patients [51,52], it is still desirable to develop safer and more effective treatment, possibly with pharmaceutical agents. The xenograft model of CAEBV generated in this study may be an excellent animal model to test novel experimental therapies for the disease. In fact, the OKT-4 antibody that depletes $CD4^+$ T cells in vivo gave a promising result implying its effectiveness as a therapeutic to CAEBV.

Materials and Methods

Ethics statement

Protocols of the experiments with materials obtained from patients with CAEBV and EBV-HLH and from control persons have been reviewed and approved by the Institutional Review Boards of the National Center for Child Health and Development and of the National Institute of Infectious diseases (NIID). Blood samples of the patients and control persons were collected after obtaining written informed consent. Protocols of the experiments with NOG mice are in accordance with the Guidelines for Animal Experimentation of the Japanese Association for Laboratory Animal Science and were approved by the Institutional Animal Care and Use Committee of NIID.

Patients with CAEBV and EBV-HLH

Characteristics of the nine patients with CAEBV and the four patients with EBV-HLH examined in this study are summarized in Table 1. Diagnosis of CAEBV and EBV-HLH was made on the basis of the published guidelines [19,53] and confirmed by identification of EBV-infected T or NK cells in their peripheral blood by flow cytometry and real-time PCR.

NOD/Shi-*scid*/IL2Rγ^{null} (NOG) mice

Mice of the NOD/Shi-*scid*/IL-2Rγ^{null} (NOG) strain [22] were obtained from the Central Institute for Experimental Animals (Kawasaki, Japan) and maintained under specific pathogen free (SPF) conditions in the animal facility of NIID, as described [22].

Transplantation of PBMC or their subfractions to NOG mice

PBMC were isolated by centrifugation on Lymphosepar I (Immuno-Biological Laboratories (IBL)) and injected intravenously to the tail vein of NOG mice at the age of 6–8 weeks. Depending on the recovery of PBMC, $1–4\times10^6$ cells were injected to 2 to 4 mice in a typical experiment with a blood sample. For transplantation with individual cellular fractions containing EBV DNA, $CD4^+$ T cells, $CD8^+$ T cells, and $CD56^+$ NK cells were separated with the IMag Cell Separation Systems (BD Pharmingen) following the protocol supplied by the manufacturer. To isolate γδT cells, $CD19^+$, $CD4^+$, $CD8^+$, $CD56^+$, and $CD14^+$ cells were serially removed from PBMC by the IMag Cell Separation Systems. From the remaining $CD19^-CD4^-CD8^-CD56^-CD14^-$ population, $CD3^+$ cells were positively selected by the same kit and defined as the γδT cell fraction. To transplant PBMC lacking individual immunophenotypic subsets, $CD19^+$, $CD4^+$, $CD8^+$, $CD56^+$ or $CD14^+$ cells were removed from PBMC by the IMag Cell Separation Systems and the remaining cells were injected to mice. To prepare PBMC lacking γδT cells, $CD19^+$, $CD4^+$, $CD8^+$, $CD56^+$, and $CD14^+$ cells isolated from PBMC in the process of obtaining γδT cell fraction (see above) were pooled and mixed with the $CD19^-CD4^-CD8^-CD56^-CD14^-$ cells that did not react with anti-CD3 antibody. For complementation experiments, an EBV-containing cell fraction and the $CD4^+$ cell fraction were isolated from a sample of PBMC as described above and the mixture of these two fractions were injected to NOG mice. The approximate numbers of injected cells are shown in Table 2.

Analysis of immunophenotypes and TCR repertoire expression by flow cytometry

PBMC isolated from the patients and the recipient NOG mice as described above were incubated for 30 min on ice with a mixture of appropriate combinations of fluorescently labeled monoclonal antibodies. After washing, five-color flow-cytometric analysis was carried out with the Cytomics FC500 analyzer (Beckman Coulter). The following directly labeled antibodies were used: phycoerythrin (PE)-conjugated antibodies to CD3, CD8, and TCRα/β, fluorescein isothiocyanate (FITC)-conjugated antibodies to CD3, CD4, CD8, CD19, TCRVγ9, TCRVδ2, and TCRγ/δ, and Phycoerythrin Texas Red (ECD)-conjugated antibody to CD45RO from Beckman Coulter; PE-conjugated antibodies to CD16, CD40, and CD40L, and FITC-conjugated antibody to CD56 from BD Pharmingen. TCR Vβ repertoire analysis was performed with the Multi-analysis TCR Vβ antibodies Kit (Beckman Coulter) according to the procedure recommended by the manufacturer.

Treatment of mice with the OKT-4 antibody

NOG mice were injected intravenously with 5×10^6 PBMC isolated from the CAEBV patient 3 (CD8 type) or 8 (NK type) and were subsequently injected intravenously with 100 μg of the OKT-4 antibody on the same day of transplantation. Additional

administration of the antibody was carried out by the same dose and route for the following three consecutive days. Peripheral blood EBV DNA load was then monitored every week. Mice were finally sacrificed four weeks post-transplantation and applied for pathological and virological analyses.

Quantification of EBV DNA by real time PCR and analysis of EBV gene expression by RT-PCR

Quantification of EBV DNA was carried out by real-time quantitative PCR assay based on the TaqMan system (Applied Biosystems), as described [54]. Analysis of EBV gene expression by RT-PCR was carried out as previously described with the following primers [55]. EBNA1: sense, gatgagcgtttgggagagctgattctgca; antisense, tcctcgtccatggttatcac. EBNA2: sense, agaggaggtggtaagcggttc; antisense, tgacgggtttccaagactatcc. LMP1: sense, ctctccttctcctcctcttg; antisense, caggagggtgatcatcagta. LMP2A: sense, atgactcatctcaacacata; antisense, catgttaggcaaattgcaaa. LMP2B: sense, cagtgtaatctgcacaaaga; antisense, catgttaggcaaattgcaaa. EBER1: sense, agcaccctacgctgccctaga; antisense, aaaacatgcggaccaccagc. Cp-EBNA1: sense,cactacaagacctacgcctctccattcatc; anti sense, ttcggtctcccctaggccctg. Wp/Cp-EBNA1: sense, tcagagcgccaggagtccacacaaat; antisense, ttcggtctcccctaggccctg. Qp-EBNA1: sense, aggcgcgggatagcgtgcgctaccgga; antisense, tcctcgtccatggttatcac. RT-PCR primers for β-actin were purchased from Takara (Osaka, Japan).

Histopathology, EBER ISH, and immunohistochemistry

Tissue samples were fixed in 10% buffered formalin, embedded in paraffin, and stained with hematoxylin and eosin. For phenotypic analysis of engrafted lymphocytes, immunostaining for CD3, CD8 (Nichirei), CD45RO, and CD20 (DAKO) was performed on paraffin sections. EBV was detected by in situ hybridization (ISH) with EBV small RNA (EBER) probe. Immunohistochemistry and ISH were performed on an automated stainer (BENCHMARK XT, Ventana Medical Systems) according to the manufacturer's recommendations. To determine the cell lineage of EBV infected cells, paraffin sections were applied to double staining with EBER ISH and immunohistochemistry. Immediately following EBER ISH, immunostaining for CD45RO or CD20 was performed. Photomicrographs was acquired with a OLYMPUS BX51 microscope equipped with 40x/0.75 and 20x/0.50 Uplan Fl objective lens, a Pixera Penguin 600CL digital camera (Pixera), and Viewfinder 3.01 (Pixera) for white balance, contrast, and brightness correction.

Quantification of cytokines

The levels of human IL-8, IFN-γ, and RANTES in plasma samples were measured with the Enzyme-linked immunosorbent assay (ELISA) kit provided by R&D Systems following instructions provided by the manufacturer.

Accession numbers

The Swiss-Prot accession numbers for the proteins described in this article are as follows: P13501 for RANTES; P10145 for IL-8; P01579 for IFN-γ; P03211 for EBNA1; P12978 for EBNA2; P12977 for EBNA3; P03230 for LMP1; and Q66562 for LMP2. The DDBJ accession number for EBER is AJ315772.

Supporting Information

Figure S1 Changes in the body weight of NOG mice transplanted with PBMC derived from patients with CAEBV or EBV-HLH. Body weight of the five CAEBV mice shown in Figure 1A (transplanted with PBMC from the patient 1, 3, 5, and 9, and with the $CD4^+$ fraction from the patient 1, respectively) and two EBV-HLH mice shown in Figure 6A (both transplanted with PBMC from the patient 11) were recorded weekly.
(TIF)

Figure S2 Histopathological analysis of a control NOG mouse. A. a NOG mouse without xenograft. A 20-week old female NOG mouse was sacrificed and examined as a reference. No human cells are identified in these tissues. Upper panels: liver tissue was stained with hematoxylin-eosin (HE), antibodies specific to human CD3 or CD20, or by ISH with an EBER probe; the rightmost panel is a double staining with EBER and human CD45RO. Bottom panels: EBER ISH in the spleen, kidney, and small intestine. B. a NOG mouse transplanted with PBMC of a healthy EBV carrier. A six-week old female NOG mouse was transplanted with 5×10^6 PBMC isolated from a normal EBV-seropositive person and sacrificed at eight weeks post-transplantation for histological analysis. Liver and Spleen tissues were stained with HE, antibodies specific to human CD3 or CD20, or by ISH with an EBER probe. No EBER-positive cells were identified in these tissues.Original magnification is ×200 for both A and B.
(TIF)

Table S1 EBV DNA load in lymphocyte subsets of a patient with CAEBV and a corresponding mouse derived from her PBMC.
(DOC)

Table S2 EBV DNA load in lymphocyte subsets of a patient with EBV-HLH and a corresponding mouse derived from his PBMC.
(DOC)

Acknowledgments

We thank Kumiko Tanaka, Ken Watanabe, and Miki Katayama for technical assistance.

Author Contributions

Conceived and designed the experiments: KI MY NS NY SF. Performed the experiments: KI MY AN FK SI HN. Analyzed the data: KI MY AN SF. Contributed reagents/materials/analysis tools: AA TM SO MI OM JK. Wrote the paper: KI SF.

References

1. Rickinson AB, Kieff ED (2007) Epstein-Barr virus. In: Knipe DM, Howley PM, eds. Fields Virology 5. ed. Philadelphia: Lippincott Williams and Wilkins. pp 2655–2700.
2. Kieff ED, Rickinson AB (2007) Epstein-Barr virus and its replication. In: Knipe DM, Howley PM, eds. Fields Virology. Philadelphia: Lippincott Williams and Wilkins. pp 2603–2654.
3. Fujiwara S, Ono Y (1995) Isolation of Epstein-Barr virus-infected clones of the human T-cell line MT-2: use of recombinant viruses with a positive selection marker. J Virol 69: 3900–3903.
4. Watry D, Hedrick JA, Siervo S, Rhodes G, Lamberti JJ, et al. (1991) Infection of human thymocytes by Epstein-Barr virus. J Exp Med 173: 971–980.
5. Kikuta H, Sakiyama Y, Matsumoto S, Oh-Ishi T, Nakano T, et al. (1993) Fatal Epstein-Barr virus-associated hemophagocytic syndrome. Blood 82: 3259–3264.
6. Kawaguchi H, Miyashita T, Herbst H, Niedobitek G, Asada M, et al. (1993) Epstein-Barr virus-infected T lymphocytes in Epstein-Barr virus-associated hemophagocytic syndrome. J Clin Invest 92: 1444–1450.
7. Kawa-Ha K, Ishihara S, Ninomiya T, Yumura-Yagi K, Hara J, et al. (1989) CD3-negative lymphoproliferative disease of granular lymphocytes containing Epstein-Barr viral DNA. J Clin Invest 84: 51–55.
8. Jones JF, Shurin S, Abramowsky C, Tubbs RR, Sciotto CG, et al. (1988) T-cell lymphomas containing Epstein-Barr viral DNA in patients with chronic Epstein-Barr virus infections. N Engl J Med 318: 733–741.

9. Kikuta H, Taguchi Y, Tomizawa K, Kojima K, Kawamura N, et al. (1988) Epstein-Barr virus genome-positive T lymphocytes in a boy with chronic active EBV infection associated with Kawasaki-like disease. Nature 333: 455–457.
10. Ishihara S, Tawa A, Yumura-Yagi K, Murata M, Hara J, et al. (1989) Clonal T-cell lymphoproliferation containing Epstein-Barr (EB) virus DNA in a patient with chronic active EB virus infection. Jpn J Cancer Res 80: 99–101.
11. Jaffe ES (2009) The 2008 WHO classification of lymphomas: implications for clinical practice and translational research. Hematology Am Soc Hematol Educ Program 2009: 523–531.
12. Okano M (2002) Overview and problematic standpoints of severe chronic active Epstein-Barr virus infection syndrome. Crit Rev Oncol Hematol 44: 273–282.
13. Straus SE (1992) Acute progressive Epstein-Barr virus infections. Annu Rev Med 43: 437–449.
14. Kimura H (2006) Pathogenesis of chronic active Epstein-Barr virus infection: is this an infectious disease, lymphoproliferative disorder, or immunodeficiency? Rev Med Virol 16: 251–261.
15. Kimura H, Morishima T, Kanegane H, Ohga S, Hoshino Y, et al. (2003) Prognostic factors for chronic active Epstein-Barr virus infection. J Infect Dis 187: 527–533.
16. Tsuge I, Morishima T, Kimura H, Kuzushima K, Matsuoka H (2001) Impaired cytotoxic T lymphocyte response to Epstein-Barr virus-infected NK cells in patients with severe chronic active EBV infection. J Med Virol 64: 141–148.
17. Sugaya N, Kimura H, Hara S, Hoshino Y, Kojima S, et al. (2004) Quantitative analysis of Epstein-Barr virus (EBV)-specific CD8+ T cells in patients with chronic active EBV infection. J Infect Dis 190: 985–988.
18. Aoukaty A, Lee IF, Wu J, Tan R (2003) Chronic active Epstein-Barr virus infection associated with low expression of leukocyte-associated immunoglobulin-like receptor-1 (LAIR-1) on natural killer cells. J Clin Immunol 23: 141–145.
19. Henter JI, Horne A, Arico M, Egeler RM, Filipovich AH, et al. (2007) HLH-2004: Diagnostic and therapeutic guidelines for hemophagocytic lymphohistiocytosis. Pediatr Blood Cancer 48: 124–131.
20. Lay JD, Tsao CJ, Chen JY, Kadin ME, Su IJ (1997) Upregulation of tumor necrosis factor-alpha gene by Epstein-Barr virus and activation of macrophages in Epstein-Barr virus-infected T cells in the pathogenesis of hemophagocytic syndrome. J Clin Invest 100: 1969–1979.
21. Imashuku S, Hibi S, Ohara T, Iwai A, Sako M, et al. (1999) Effective control of Epstein-Barr virus-related hemophagocytic lymphohistiocytosis with immunochemotherapy. Histiocyte Society. Blood 93: 1869–1874.
22. Ito M, Hiramatsu H, Kobayashi K, Suzue K, Kawahata M, et al. (2002) NOD/SCID/gamma(c)(null) mouse: an excellent recipient mouse model for engraftment of human cells. Blood 100: 3175–3182.
23. Shultz LD, Lyons BL, Burzenski LM, Gott B, Chen X, et al. (2005) Human lymphoid and myeloid cell development in NOD/LtSz-scid IL2R gamma null mice engrafted with mobilized human hemopoietic stem cells. J Immunol 174: 6477–6489.
24. Strowig T, Gurer C, Ploss A, Liu YF, Arrey F, et al. (2009) Priming of protective T cell responses against virus-induced tumors in mice with human immune system components. J Exp Med 206: 1423–1434.
25. Watanabe S, Terashima K, Ohta S, Horibata S, Yajima M, et al. (2007) Hematopoietic stem cell-engrafted NOD/SCID/IL2Rgamma null mice develop human lymphoid systems and induce long-lasting HIV-1 infection with specific humoral immune responses. Blood 109: 212–218.
26. Yajima M, Imadome K, Nakagawa A, Watanabe S, Terashima K, et al. (2008) A new humanized mouse model of Epstein-Barr virus infection that reproduces persistent infection, lymphoproliferative disorder, and cell-mediated and humoral immune responses. J Infect Dis 198: 673–682.
27. Traggiai E, Chicha L, Mazzucchelli L, Bronz L, Piffaretti JC, et al. (2004) Development of a human adaptive immune system in cord blood cell-transplanted mice. Science 304: 104–107.
28. Melkus MW, Estes JD, Padgett-Thomas A, Gatlin J, Denton PW, et al. (2006) Humanized mice mount specific adaptive and innate immune responses to EBV and TSST-1. Nat Med 12: 1316–1322.
29. Baenziger S, Tussiwand R, Schlaepfer E, Mazzucchelli L, Heikenwalder M, et al. (2006) Disseminated and sustained HIV infection in CD34+ cord blood cell-transplanted Rag2-/-gamma c-/- mice. Proc Natl Acad Sci U S A 103: 15951–15956.
30. Zhang L, Kovalev GI, Su L (2007) HIV-1 infection and pathogenesis in a novel humanized mouse model. Blood 109: 2978–2981.
31. Dewan MZ, Watanabe M, Ahmed S, Terashima K, Horiuchi S, et al. (2005) Hodgkin's lymphoma cells are efficiently engrafted and tumor marker CD30 is expressed with constitutive nuclear factor-kappaB activity in unconditioned NOD/SCID/gammac(null) mice. Cancer Sci 96: 466–473.
32. Ishikawa F, Yoshida S, Saito Y, Hijikata A, Kitamura H, et al. (2007) Chemotherapy-resistant human AML stem cells home to and engraft within the bone-marrow endosteal region. Nat Biotechnol 25: 1315–1321.
33. Durig J, Ebeling P, Grabellus F, Sorg UR, Mollmann M, et al. (2007) A novel nonobese diabetic/severe combined immunodeficient xenograft model for chronic lymphocytic leukemia reflects important clinical characteristics of the disease. Cancer Res 67: 8653–8661.
34. Nakagawa A, Ito M, Saga S (2002) Fatal cytotoxic T-cell proliferation in chronic active Epstein-Barr virus infection in childhood. Am J Clin Pathol 117: 283–290.
35. Nagata H, Konno A, Kimura N, Zhang Y, Kimura M, et al. (2001) Characterization of novel natural killer (NK)-cell and gammadelta T-cell lines established from primary lesions of nasal T/NK-cell lymphomas associated with the Epstein-Barr virus. Blood 97: 708–713.
36. Imai S, Sugiura M, Oikawa O, Koizumi S, Hirao M, et al. (1996) Epstein-Barr virus (EBV)-carrying and -expressing T-cell lines established from severe chronic active EBV infection. Blood 87: 1446–1457.
37. Yoshioka M, Ishiguro N, Ishiko H, Ma X, Kikuta H, et al. (2001) Heterogeneous, restricted patterns of Epstein-Barr virus (EBV) latent gene expression in patients with chronic active EBV infection. J Gen Virol 82: 2385–2392.
38. Kimura H, Hoshino Y, Hara S, Sugaya N, Kawada J, et al. (2005) Differences between T cell-type and natural killer cell-type chronic active Epstein-Barr virus infection. J Infect Dis 191: 531–539.
39. Xu J, Ahmad A, Jones JF, Dolcetti R, Vaccher E, et al. (2000) Elevated serum transforming growth factor beta1 levels in Epstein-Barr virus-associated diseases and their correlation with virus-specific immunoglobulin A (IgA) and IgM. J Virol 74: 2443–2446.
40. Ohga S, Nomura A, Takada H, Ihara K, Kawakami K, et al. (2001) Epstein-Barr virus (EBV) load and cytokine gene expression in activated T cells of chronic active EBV infection. J Infect Dis 183: 1–7.
41. Hayashi K, Ohara N, Teramoto N, Onoda S, Chen HL, et al. (2001) An animal model for human EBV-associated hemophagocytic syndrome: herpesvirus papio frequently induces fatal lymphoproliferative disorders with hemophagocytic syndrome in rabbits. Am J Pathol 158: 1533–1542.
42. Veronese ML, Veronesi A, D'Andrea E, Del Mistro A, Indraccolo S, et al. (1992) Lymphoproliferative disease in human peripheral blood mononuclear cell-injected SCID mice. I. T lymphocyte requirement for B cell tumor generation. J Exp Med 176: 1763–1767.
43. Johannessen I, Asghar M, Crawford DH (2000) Essential role for T cells in human B-cell lymphoproliferative disease development in severe combined immunodeficient mice. Br J Haematol 109: 600–610.
44. Sutkowski N, Palkama T, Ciurli C, Sekaly RP, Thorley-Lawson DA, et al. (1996) An Epstein-Barr virus-associated superantigen. J Exp Med 184: 971–980.
45. Anagnostopoulos I, Hummel M, Kreschel C, Stein H (1995) Morphology, immunophenotype, and distribution of latently and/or productively Epstein-Barr virus-infected cells in acute infectious mononucleosis: implications for the interindividual infection route of Epstein-Barr virus. Blood 85: 744–750.
46. Hudnall SD, Ge Y, Wei L, Yang NP, Wang HQ, et al. (2005) Distribution and phenotype of Epstein-Barr virus-infected cells in human pharyngeal tonsils. Mod Pathol 18: 519–527.
47. Hislop AD, Taylor GS, Sauce D, Rickinson AB (2007) Cellular responses to viral infection in humans: lessons from Epstein-Barr virus. Annu Rev Immunol 25: 587–617.
48. Katano H, Ali MA, Patera AC, Catalfamo M, Jaffe ES, et al. (2004) Chronic active Epstein-Barr virus infection associated with mutations in perforin that impair its maturation. Blood 103: 1244–1252.
49. van Rijn RS, Simonetti ER, Hagenbeek A, Hogenes MC, de Weger RA, et al. (2003) A new xenograft model for graft-versus-host disease by intravenous transfer of human peripheral blood mononuclear cells in RAG2-/- gammac-/- double-mutant mice. Blood 102: 2522–2531.
50. Ito R, Katano I, Kawai K, Hirata H, Ogura T, et al. (2009) Highly sensitive model for xenogenic GVHD using severe immunodeficient NOG mice. Transplantation 87: 1654–1658.
51. Kawa K, Sawada A, Sato M, Okamura T, Sakata N, et al. (2011) Excellent outcome of allogeneic hematopoietic SCT with reduced-intensity conditioning for the treatment of chronic active EBV infection. Bone Marrow Transplant 46: 77–83.
52. Sato E, Ohga S, Kuroda H, Yoshiba F, Nishimura M, et al. (2008) Allogeneic hematopoietic stem cell transplantation for Epstein-Barr virus-associated T/natural killer-cell lymphoproliferative disease in Japan. Am J Hematol 83: 721–727.
53. Okano M, Kawa K, Kimura H, Yachie A, Wakiguchi H, et al. (2005) Proposed guidelines for diagnosing chronic active Epstein-Barr virus infection. Am J Hematol 80: 64–69.
54. Kimura H, Morita M, Yabuta Y, Kuzushima K, Kato K, et al. (1999) Quantitative analysis of Epstein-Barr virus load by using a real-time PCR assay. J Clin Microbiol 37: 132–136.
55. Nakamura H, Iwakiri D, Ono Y, Fujiwara S (1998) Epstein-Barr-virus-infected human T-cell line with a unique pattern of viral-gene expression. Int J Cancer 76: 587–594.

Cancer Letters xxx (2013) xxx–xxx

Contents lists available at SciVerse ScienceDirect

Cancer Letters

journal homepage: www.elsevier.com/locate/canlet

Potent antitumor activity of zoledronic acid-induced Vγ9Vδ2 T cells against primary effusion lymphoma

Hiroki Goto [a], Kouki Matsuda [a], Pattaravadee Srikoon [a], Ryusho Kariya [a], Shinichiro Hattori [a], Manabu Taura [a], Harutaka Katano [b], Seiji Okada [a,*]

[a] Division of Hematopoiesis, Center for AIDS Research, Kumamoto University, Honjo, Kumamoto, Japan
[b] Department of Pathology, National Institute of Infectious Diseases, Toyama, Shinjuku, Tokyo, Japan

ARTICLE INFO

Article history:
Received 1 October 2012
Received in revised form 10 December 2012
Accepted 25 December 2012
Available online xxxx

Keywords:
AIDS
Primary effusion lymphoma
Vγ9Vδ2 T cell
Zoledronic acid

ABSTRACT

Primary effusion lymphoma (PEL) is a subtype of aggressive and resistant non-Hodgkin lymphoma that occurs predominantly in patients with advanced AIDS. In this study, we examined the antitumor activity of zoledronic acid (Zol)-induced Vγ9Vδ2 T cells against PEL cells *in vitro* and *in vivo*. Vγ9Vδ2 T cells recognized endogenous mevalonate metabolites and MICA/B of PEL cell lines, inducing cytotoxicity via granule exocytosis and TRAIL-mediated pathway. Vγ9Vδ2 T cells suppressed the development of PEL cells and existed in a PEL xenograft mouse model. These results show that immunotherapy with Zol-induced Vγ9Vδ2 T cells could demonstrate an efficient strategy for PEL.

1. Introduction

Primary effusion lymphoma (PEL) is an infrequent and distinct entity of aggressive non-Hodgkin B-cell lymphoma that shows serous lymphomatous effusion in body cavities (pleura, peritoneum and pericardium) and is universally associated with Kaposi sarcoma-associated herpes virus/human herpes virus-8 (KSHV/HHV-8) [1,2]. PEL is diagnosed most commonly in patients with HIV/AIDS, accounting for 4% of all non-Hodgkin lymphomas in this population [3]. The lack of optimal therapy combined with the aggressive nature of PEL results in a short median survival of less than 6 months [4]. There is therefore an urgent need for the development of new therapeutics.

Human γδ T cells account for 1–10% $CD3^+$ cells in the peripheral blood of healthy adults [5]. The majority expressed Vγ9Vδ2 T cell receptor (TCR) [6]. Unlike αβ T cells, Vγ9Vδ2 T cells recognize non-peptidic antigens without antigen processing and major histocompatibility complex (MHC) restriction. There is growing evidence of the antitumor activity of Vγ9Vδ2 T cells against a large range of tumor types, including hematopoietic tumor cells [7].

Phosphoantigens, such as isopentenyl pyrophosphate (IPP) and the synthetic analog bromohydrin pyrophosphate (BrHPP), activate Vγ9Vδ2 T cells *in vitro*, inducing their cytotoxic activity against tumor or infected target cells [8]. Nitrogen-containing bisphosphonates (N-BPs), such as zoledronic acid (Zol), indirectly stimulate Vγ9Vδ2 T cells by inhibiting farnesyl diphosphate synthase, a key enzyme of the mevalonate pathway, causing the intracellular accumulation of IPP [9].

We expanded Vγ9Vδ2 T cells from healthy donors with Zol and evaluated the efficacy of Vγ9Vδ2 T cells against PEL cells *in vitro* and *in vivo*. Vγ9Vδ2 T cells recognized endogenous mevalonate metabolites and MHC class I-related chain A and B (MICA/B), of PEL cells. The cytotoxic activity was mediated by granule exocytosis and the tumor necrosis factor-related apoptosis-inducing ligand (TRAIL) pathway. In the *in vivo* assessment using a PEL xenograft mouse model, Vγ9Vδ2 T cells inhibited the growth and invasion of PEL cells and were found in the spleen and peripheral blood of the treated mice.

These results show the effect of Vγ9Vδ2 T cell-based immunotherapy against PEL cells and provide insight into the role of Vγ9Vδ2 T cells in tumor immunity for PEL.

2. Materials and methods

2.1. Cell lines and reagents

Human PEL cell lines, BCBL-1 (obtained through the AIDS Research and Reference Reagent Program, Division of AIDS, NIAID, NIH), BC-1 (purchased from ATCC, Rockville, MD), BC-3 (purchased from ATCC) and Burkitt lymphoma cell line, Daudi (obtained from RIKEN Cell Bank, Tsukuba, Japan) were maintained in RPMI 1640 supplemented with 10% heat-inactivated fetal bovine serum (FBS), penicillin (100 U/ml) and streptomycin (100 μg/ml) in a humidified incubator at 37 °C and 5% CO_2. Zol was obtained from Novartis Pharma AG (Basel, Switzerland).

* Corresponding author. Address: Division of Hematopoiesis, Center for AIDS Research, Kumamoto University, 2-2-1 Honjo, Chuo-ku, Kumamoto 860-0811, Japan. Tel.: +81 96 373 6522; fax: +81 96 373 6523.
E-mail address: okadas@kumamoto-u.ac.jp (S. Okada).

0304-3835/$ - see front matter © 2013 Elsevier Ireland Ltd. All rights reserved.
http://dx.doi.org/10.1016/j.canlet.2012.12.021

Please cite this article in press as: H. Goto et al., Potent antitumor activity of zoledronic acid-induced Vγ9Vδ2 T cells against primary effusion lymphoma, Cancer Lett. (2013), http://dx.doi.org/10.1016/j.canlet.2012.12.021

2.2. Human Vγ9Vδ2 T cell preparations and culture

Informed consent was obtained for the collection of peripheral blood from healthy volunteers. Peripheral blood mononuclear cells (PBMCs) were separated individually from blood samples donated by three healthy volunteers using Pancoll (PAN Biotech GmbH, Aidenbach, Germany). PBMCs were stimulated with 1 μM Zol and cultured for 14 days at 37 °C in a humidified atmosphere of 5% CO_2. Medium consisted of RPMI 1640 supplemented with 10% heat-inactivated FBS, penicillin (100 U/ml) and streptomycin (100 μg/ml). On day 1, 5, 9, and 13, 100 U/ml interleukin-2 (IL-2) was added to the culture. On day 14, γδ T cells were isolated from expanded γδ T cells by negative selection using γδ T-cell isolation kits (Miltenyi Biotec, Bergisch Gladbach, Germany), as per the manufacturer's instructions. After isolation, the percentage of γδ T cells was more than 95.0%.

2.3. Flow cytometry

Cells were stained with the following monoclonal antibody (mAb): TCR Vγ9-phycoerythrin (PE), TCR Vδ2-fluorescein isothiocyanate (FITC), DR4(TRAIL-R1)-PE, DR5(TRAIL-R2)-PE, CD107a-PE, human CD45-pacific blue (PB), mouse CD45-Alexafluor 700 (AF 700), MICA/B-Alexafluor 647 (AF 647) from BioLegend (San Diego, CA); CD138-FITC from e-Bioscience (San Diego, CA); Fas(CD95)-PE from BD PharMingen (San Diego, CA). To determine perforin expression, cells were fixed with 1% paraformaldehyde and permeabilized with 0.1% saponin. The frequency of degranulating Vγ9Vδ2 T cells was quantified by measuring CD107a expression. Vγ9Vδ2 T cells were co-incubated with PEL cell lines as an effector to target a cell (E:T) ratio of 1:1 for 1 h at 37 °C in 5% CO_2, after which brefeldin A (Sigma–Aldrich, St. Louis, MO) was added at a final concentration of 10 μg/ml and incubated for an additional 4 h at 37 °C in 5% CO_2. Subsequently, the cells were washed and stained with TCR Vδ2-FITC. After staining, cells were washed twice, resuspended in staining medium (PBS with 3% FBS and 0.05% sodium azide), and immediately analyzed on an LSR II flow cytometer (BD Bioscience, San Jose, CA). Data were analyzed with FlowJo software (Tree Star, San Jose, CA).

2.4. Tetrazolium dye methylthiotetrazole (MTT) assay

The antiproliferative activities of Zol against PEL cell lines were measured by the methylthiotetrazole (MTT) method (Sigma–Aldrich). Briefly, 2×10^4 cells were incubated in triplicate in a 96-well microculture plate in the presence of different concentrations of Zol in a final volume of 0.1 ml for 24 h at 37 °C. Subsequently, MTT (0.5 mg/ml final concentration) was added to each well. After 3 h of additional incubation, 100 μl of a solution containing 10% SDS plus 0.01 N HCl was added to dissolve the crystals. Absorption values at 595 nm were determined with an automatic enzyme-linked immunosorbent assay (ELISA) plate reader (Multiskan; Thermo ElectronVantaa, Finland). Values were normalized to untreated (control) samples.

2.5. In vitro cytotoxicity assay and blocking studies

Purified Vγ9Vδ2 T cells were resuspended at final concentrations of 2×10^5, 1×10^6, and 2×10^6 cells/ml, and 100 μl was then added to round-bottomed polystyrene tubes together with target cells (100 μl) to obtain E:T ratios of 1:1, 5:1, and 10:1. Cytotoxicity was measured by flow cytometric analysis using CFSE and propidium iodide (PI) as previously described [10]. Briefly, 50 μl CFSE (Invitrogen, Carlsbad, CA) was added to 1 ml target cell suspension (5×10^5 cells/ml) in PBS to obtain the final concentration of 2.5 μM CFSE. The cells were incubated for 10 min at 37 °C and gently mixed every 5 min. At the end of incubation, 1 ml FBS was added to the cell suspension to stop the staining reaction, and the cells were centrifuged at 400g for 5 min at room temperature, washed twice with cold PBS, and resuspended in complete medium. Control tubes containing only labeled target cells and effector cells were also prepared to establish background levels of cell death. Tubes were gently mixed, centrifuged at 300g for 2 min, and incubated at 37 °C in 5% CO_2 for 4 h.

At the end of the incubation period, 300 μl complete medium and 1 μl of 1 mg/ml PI were added to each tube for 15 min before acquisition on LSR II cytometer. The measurement of cytotoxic activity was based on the degree of reduction of viable target cells with the ability to retain CFSE and exclude PI ($CFSE^{high}$ PI^-). To inhibit perforin-mediated cytotoxicity, Vγ9Vδ2 T cells were incubated with 300 nM concanamycin A (CMA) (A.G. Scientific, Inc., San Diego, CA) for 30 min at 37 °C prior to coculture, without further washing. To inhibit recognition of endogenous mevalonate metabolites, PEL cells were incubated with 25 μM mevastatin (Mev) (Sigma–Aldrich) for 60 min at 37 °C prior to coculture, without further washing. For blocking mAbs, anti-FasL (clone NOK-1), anti-TRAIL (clone RIK-2), anti-MICA/B (clone 6D4), mouse IgG1 Isotype Ctrl (clone MG1-45), mouse IgG2a Isotype Ctrl (clone MOPC-173) (Biolegend) were used to evaluate the mechanisms of Vγ9Vδ2 T cell-mediated cytotoxicity of PEL cell lines at the final concentration of 10 μg/ml. Vγ9Vδ2 T cells were cultured with PEL cell lines at an E:T ratio of 10:1 in the presence of CMA, Mev or blocking Abs. Pretreatment of Vγ9Vδ2 T cells or PEL cells with CMA or Mev at the concentrations used in this study did not have any cytotoxic effect.

2.6. Xenograft mouse model

NOD Rag-2-deficient (Rag-$2^{-/-}$) mice and NOD Jak3-deficient (Jak$3^{-/-}$) mice were established by crossing Rag-$2^{-/-}$ mice or Jak$3^{-/-}$ mice with the NOD strain for 10 generations, respectively. NOD Rag-2/Jak3 double-deficient (Rag-$2^{-/-}$Jak$3^{-/-}$) mice (NRJ mice) were established by crossing NOD Rag-$2^{-/-}$ mice and NOD Jak$3^{-/-}$ mice, and were housed and monitored in our animal research facility according to institutional guidelines. All experimental procedures and protocols were approved by the Institutional Animal Care and Use Committee at Kumamoto University. Eight to twelve week-old NRJ mice were intraperitoneally inoculated with 7×10^6 BCBL-1 cells or BC-3 cells suspended in 200 μl PBS. The mice were then treated with intraperitoneal injections of PBS or *ex vivo* expanded 3×10^7 Vγ9Vδ2 T cells on day 3 after cell inoculation and once a week. The mice of both groups were also treated with 2 μg Zol (on day 3) and 3000 U IL-2 (twice a week) intraperitoneally. Tumor burden was evaluated by measuring the body weight gain, the volume of ascites and the percentage of human CD45 gated $CD138^+$ cells in the spleen.

2.7. Immunohistochemistry

To investigate the expression of KSHV/HHV-8 ORF73 (LANA) protein, tissue samples were fixed with 10% neutral-buffered formalin, embedded in paraffin and cut into 4-μm sections. The sections were deparaffinized by sequential immersion in xylene and ethanol, and rehydrated in distilled water. They were then irradiated for 15 min in a microwave oven for antigen retrieval. Endogenous peroxidase activity was blocked by immersing the sections in methanol/0.6% H_2O_2 for 30 min at room temperature. Affinity-purified PA1-73N antibody [11], diluted 1:3000 in PBS/5% bovine serum albumin (BSA), was then applied, and the sections were incubated overnight at 4 °C. After washing in PBS twice, the second and third reactions and the amplification procedure were performed using kits according to the manufacturer's instructions (catalyzed signal amplification system kit; DAKO, Copenhagen, Denmark). The signal was visualized using 0.2 mg/ml diaminobenzidine and 0.015% H_2O_2 in 0.05 mol/l Tris–HCl, pH 7.6.

2.8. Statistical analysis

Data are expressed as the mean ± SD. The statistical significance of the differences observed between experimental groups was determined using Student's *t*-test, and $P < 0.05$ was considered significant.

3. Results

3.1. Proliferation of Vγ9Vδ2 T cells by Zol

Fig. 1A shows representative data of Vγ9Vδ2 T cell expansion. Consistent with other reports, Vγ9Vδ2 T cells represented a minor subset of peripheral lymphocytes (1–10%) before culture [5]. Following exposure to 1 μM Zol and IL-2 (100 U/ml, on day 1, 5, 9, 13), the percentages of Vγ9Vδ2 T cells reached up to more than 80% on day 14 (Fig. 1A). Determination of the absolute number of Vγ9Vδ2 T cells increased for 14 days and ranged from 88.0 to 134.1-fold expansion after 14 days in three normal volunteers (Fig. 1B), indicating the efficient expansion of Vγ9Vδ2 T cells by our method.

3.2. In vitro cytotoxicity of ex vivo expanded Vγ9Vδ2 T cells

Three PEL cell lines (BCBL-1, BC-1, and BC-3),the Burkitt lymphoma cell line, Daudi, and non-target cells, PBMCs, were cultured with Vγ9Vδ2 T cells at each E/T ratio (0, 1, 5 and 10) for 4 h, and cytotoxicity was measured by flow cytometric analysis using CFSE and PI as described in Materials and Methods. The percentage of specific lysis against PEL cell lines by *ex vivo* expanded Vγ9Vδ2 T cells increased in an E/T ratio-dependent manner, whereas Vγ9Vδ2 T cells had no obvious cytotoxic effect on PBMCs (Fig. 2). Vγ9Vδ2 T cells had the same levels of cytotoxicity against PEL cell lines as the standard target Daudi Burkitt lymphoma cell line, which possessed strong sensitivity to Vγ9Vδ2 T cells [12]. These findings indicated that Vγ9Vδ2 T cells killed PEL cell lines efficiently. Although N-BPs have been reported to have direct antitumor effects on several cancer cell lines via the inactivation of Ras-related proteins [13], the methylthiotetrazole assay showed that Zol did not have a direct antitumor effect against PEL cell lines with the concentrations

Please cite this article in press as: H. Goto et al., Potent antitumor activity of zoledronic acid-induced Vγ9Vδ2 T cells against primary effusion lymphoma, Cancer Lett. (2013), http://dx.doi.org/10.1016/j.canlet.2012.12.021

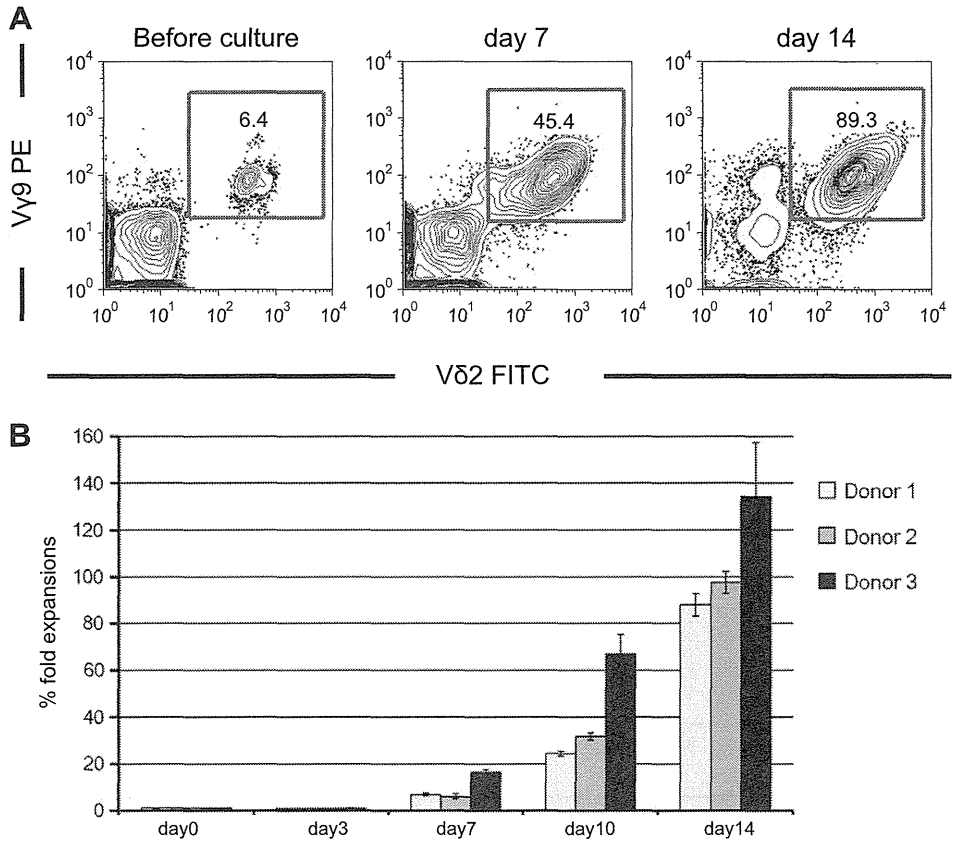

Fig. 1. *Vγ9Vδ2 T cells were generated by expanding PBMC from healthy donors with Zol and IL-2.* (A) *Representative flow cytometric profiles with the ratio of Vγ9Vδ2 T cells* before culture, on day 7, and 14. (B) Fold expansion (%) of Vγ9Vδ2 T cells following culture. Data are shown as the mean ± SD of three experiments from three healthy volunteers.

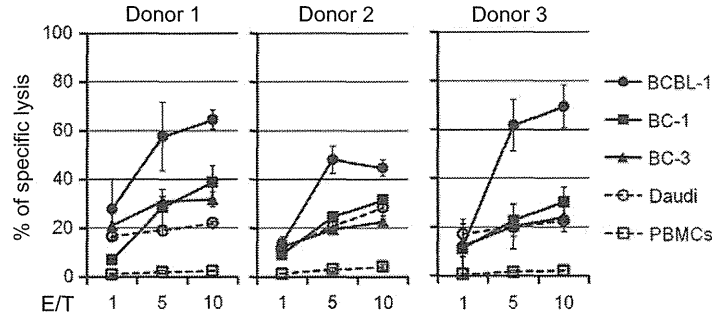

Fig. 2. Vγ9Vδ2 T cell-mediated cytotoxicity of PEL cell lines. Data are shown as the mean ± SD of three experiments from three healthy volunteers.

ranging 0–10 μM (Supplementary Fig. 1). Moreover, pretreatment of PEL cells with Zol (at concentrations up to 10 μM) for 24 h did not enhance the susceptibility to cytotoxicity by Vγ9Vδ2 T cells significantly (data not shown).

3.3. PEL cell lines constitutively express death receptors and MICA/B

To determine the possible mechanisms involved in Vγ9Vδ2 T cell-mediated cytotoxicity, we examined PEL cell surface expression of Fas (CD95), DR4 (TRAIL-R1), DR5 (TRAIL-R2) and MICA/B. As depicted in Fig. 3A, PEL cell lines constitutively expressed all these molecules, although the level of expression varied among the cell lines.

3.4. Vγ9Vδ2 T cells recognize endogenous mevalonate metabolites and MICA/B of PEL cell lines, inducing cytotoxicity via the perforin and TRAIL-mediated pathway

It has been reported that Vγ9Vδ2 T cells recognize endogenous mevalonate metabolites and NKG2D ligands, such as MICA/B, of tumor targets [8,14,15]. The mechanism of cytotoxicity includes death receptor/ligand interactions and the release of perforin/granzymes. As shown in Fig. 3B, killing-inhibition experiments using CMA, Mev and Ab against MICA/B revealed Vγ9Vδ2 T cells recognized PEL cells via endogenous metabolites (means of 34.0–65.8% inhibition) and MICA/B (means of 25.5–39.7% inhibition), and killed them by the perforin pathway (means of 28.2–43.7% inhibition). Addition of Ab against TRAIL caused significant killing

Please cite this article in press as: H. Goto et al., Potent antitumor activity of zoledronic acid-induced Vγ9Vδ2 T cells against primary effusion lymphoma, Cancer Lett. (2013), http://dx.doi.org/10.1016/j.canlet.2012.12.021

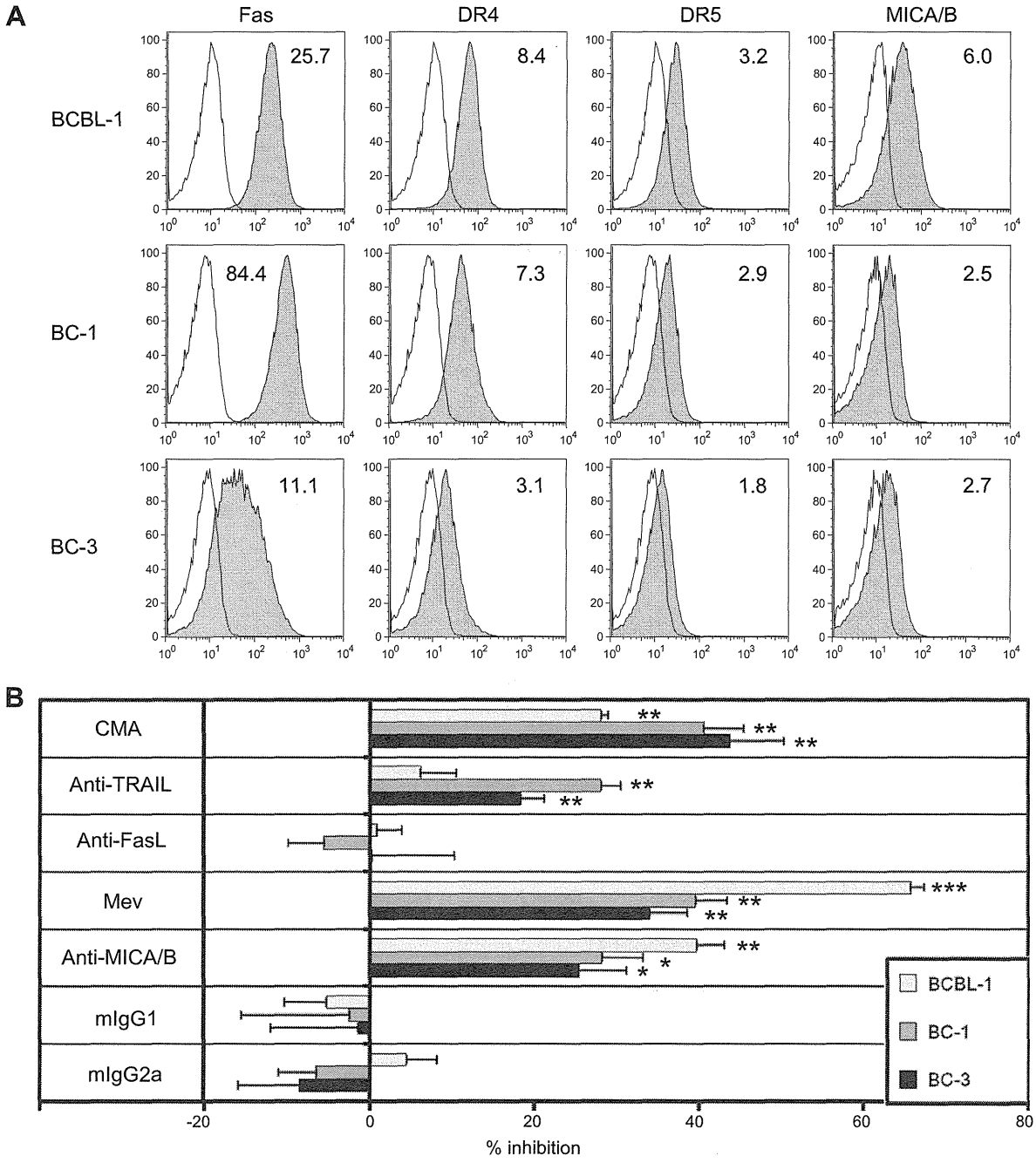

Fig. 3. Phenotype of PEL cell lines and mechanisms of Vγ9Vδ2 T cell cytotoxicity of PEL target cells. (A) Expression of Fas, DR4, DR5 and MICA/B on the surface of PEL cell lines. Numbers in histograms indicate the fold increase in the mean fluorescence intensity. (B) Vγ9Vδ2 T cells were cultured with PEL cells at an E:T ratio of 10:1 in the presence of CMA, Mev or blocking Abs to FasL, TRAIL, MICA/B or isotype Ctrl. Data are shown as the mean ± SD of three experiments from one healthy volunteer. $^{*}P < 0.05$; $^{**}P < 0.01$; $^{***}P < 0.001$ when compared with cytotoxicity carried out in the absence of inhibitors.

inhibition of BC-1 (mean of 28.1% inhibition) and BC-3 (mean of 18.4% inhibition), respectively, but had no significant effect on the death of BCBL-1 (mean of 6.2% inhibition), indicating that the cytotoxicity of Vγ9Vδ2 T cells against PEL cells was partially mediated by the TRAIL pathway. Addition of Ab against FasL or isotype Ctrl caused no significant inhibition against all tested PEL cells. Next, we evaluated the expression of CD107a (lysosome-associated membrane protein-1), a marker associated with the degranulation of cytotoxic $CD8^+$ T cell [16] and NK cell [17]. Following coculture of Vγ9Vδ2 T cells with PEL cell lines, CD107a expression on the surface of Vγ9Vδ2 T cells was up-regulated 2.1- to 2.8-fold, indicating the degranulation of Vγ9Vδ2 T cells against PEL cells (Fig. 4).

3.5. In vivo effect of Vγ9Vδ2 T cells

To evaluate the potential of the immunotherapy strategy, we used a previously established model of PEL transplantation into severe immunodeficient, NOD/Rag-2/Jak3-deficient (NRJ) mice [18]. NRJ mice were inoculated intraperitoneally with 7×10^6 BCBL-1 cells or BC-3 cells. BCBL-1 or BC-3 produced profuse ascites within 4 weeks of inoculation (Fig. 5A). Then, 3×10^7 Vγ9Vδ2 T cells or PBS alone was administrated via intraperitoneal injection on day 3 after cell inoculation and once a week; 2 μg Zol (on day 3) and 3000 U IL-2 (twice a week) were also injected intraperitoneally. Vγ9Vδ2 T cell-treated mice seemed to show no apparent change,

Please cite this article in press as: H. Goto et al., Potent antitumor activity of zoledronic acid-induced Vγ9Vδ2 T cells against primary effusion lymphoma, Cancer Lett. (2013), http://dx.doi.org/10.1016/j.canlet.2012.12.021

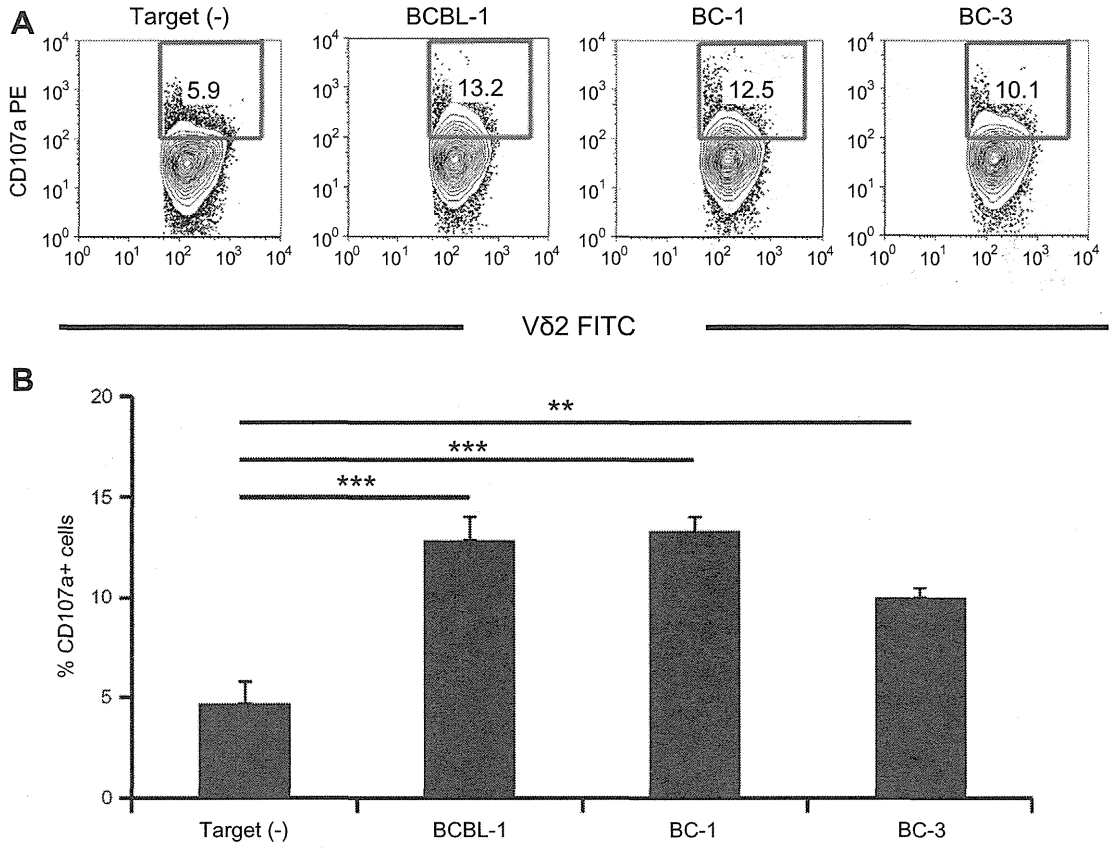

Fig. 4. Expression of CD107a of γδ T cells following coculture with PEL cells. (A) Representative flow cytometric profiles of CD107a$^+$ cells among Vδ2$^+$ cells following coculture with PEL cell lines. (B) Levels of CD107a$^+$ cells among Vδ2$^+$ cells following coculture with or without PEL cell lines at an E:T ratio of 1:1. Data are shown as the mean ± SD of three experiments from one healthy volunteer. $^{**}P < 0.01$; $^{***}P < 0.001$ when compared with CD107a expression of Vδ2$^+$ cells in the absence of PEL cells.

and the body weight gain of untreated mice significantly increased compared to that of Vγ9Vδ2 T cell-treated mice on day 31 (7.5 ± 2.7 g *vs.* 4.1 ± 3.1 g in BCBL-1 xenografts, 6.5 ± 2.6 g *vs.* 2.8 ± 2.0 g in BC-3 xenografts, $n = 7$ for each group; Fig. 5B). The body weight gain of treated mice was not significantly different from that of age matched control mice on day 31. In addition, the volume of ascites was significantly lower than in untreated mice on day 31 (2.8 ± 1.0 ml *vs.* 0.9 ± 1.0 ml in BCBL-1 xenografts, 3.3 ± 1.5 ml *vs.* 0.6 ± 0.8 ml in BC-3 xenografts, $n = 7$ for each group; Fig. 5C).

Organ invasion by PEL cells on day 31 was evaluated by hematoxylin–eosin staining and LANA immunostaining. We found that mice inoculated intraperitoneally with BCBL-1 exhibited invasion into the liver and lung without macroscopic lymphoma formation (Fig. 6). The number of LANA-positive cells in Vγ9Vδ2 T cell-treated mice was significantly reduced (0–1 cells per field magnification, ×40) compared to untreated mice (50–100 cells per field magnification, ×40). The presence of BCBL-1 cells and Vγ9Vδ2 T cells was assessed by flow cytometry on day 31. The ratio of BCBL-1 cells in the spleen of treated mice was reduced significantly compared with untreated mice (0.1 ± 0.1% *vs.* 2.6 ± 1.8%, $n = 5$ for each group, $P < 0.05$; Fig. 7A and B).

These results demonstrated that Vγ9Vδ2 T cells significantly inhibit the growth and infiltration of PEL cells *in vivo* and could be a potential therapy for patients with PEL.

3.6. Engraftment of Vγ9Vδ2 T cells in the xenograft model

The percentage of Vγ9Vδ2 T cells in treated mice averaged 4.3 ± 2.6% in the spleen (Fig. 7A and C) and 2.2 ± 2.0% in the peripheral blood on day 31. Vγ9Vδ2 T cells were present and persisted in the xenograft model in the spleen and peripheral blood of NRJ mice for at least 7 days after the final i.p. administration of Vγ9Vδ2 T cells. The xenograft model using NRJ mice could be a potential tool to evaluate not only the therapeutic effect of PEL cells but also the dynamics of Vγ9Vδ2 T cells *in vivo*.

4. Discussion

PEL is characterized by clinical aggressiveness and resistance to conventional chemotherapy; therefore, there is a need to develop new therapies. Recently, several new therapeutic strategies for PEL have been proposed. These strategies involve activating TRAIL-mediated apoptosis by IFN-α and azidothymidine [19,20], inhibition of NF-κB [21], or inducing lytic replication of HHV-8 while blocking virus production [22]. Despite *in vitro* and *in vivo* studies of therapy for PEL, to date there is no standard treatment.

Although Vγ9Vδ2 T cells represent a minor subset (1–10%) of human peripheral lymphocytes, they exhibit potent MHC-unrestricted lytic activity against different tumor cell and play a crucial role in tumor immunosurveillance. Vγ9Vδ2 T cell number and reactivity are rapidly impaired after HIV-1 infection [23]; however, highly active antiretroviral therapy (HAART) is able to restore Vγ9Vδ2 T cell number and function [24]. HIV-mediated depletion of Vγ9Vδ2 T cells has the possibility to contribute to HIV-related malignancy [25]. Induction of Vγ9Vδ2 T cells is considered to be potential immunotherapy against HIV-related malignancies including PEL. Zoledronic acid (Zol), currently the most potent third generation bisphosphonate, is safe and widely used to treat

Please cite this article in press as: H. Goto et al., Potent antitumor activity of zoledronic acid-induced Vγ9Vδ2 T cells against primary effusion lymphoma, Cancer Lett. (2013), http://dx.doi.org/10.1016/j.canlet.2012.12.021

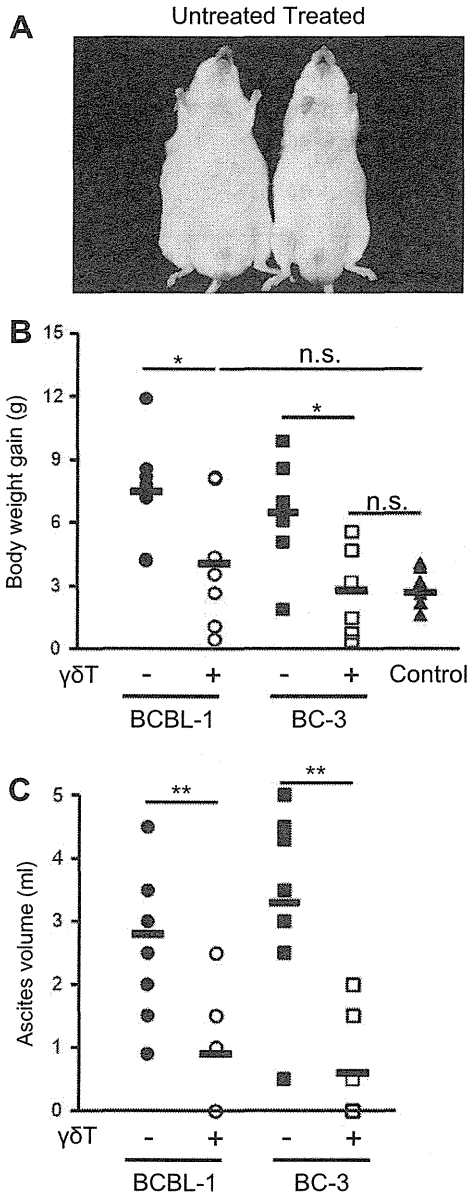

Fig. 5. Treatment of NOD/Rag-2/Jak3-deficient mice with Vγ9Vδ2 T cells suppresses the development of PEL *in vivo*. (A) Photograph of Vγ9Vδ2 T cell-treated and -untreated ascites-bearing mice 31 days after inoculation with BCBL-1 intraperitoneally. (B) Body weight gain of mice 31 days after inoculation with BCBL-1 cells or BC-3 cells in Vγ9Vδ2 T cell-treated or untreated mice is shown as the mean ± SD of seven mice. Control indicates the group of age matched mice without PEL cell injection and Zol/IL-2 treatment. (C) Volume of ascites 31 days after inoculation with BCBL-1 cells or BC-3 cells in the mice is shown as the mean ± SD of seven mice. $^{*}P < 0.05$; $^{**}P < 0.01$ when compared with body weight gain or ascites volume.

osteoporosis, hypercalcemia and bone metastases in patients with breast and prostate cancer [26]. Zol induces Vγ9Vδ2 T cell expansion more efficiently by inhibiting farnesyl diphosphate synthase compared with other bisphosphonates [27]. In this study, we investigated the cytotoxic activity of Zol-induced Vγ9Vδ2 T cells against PEL cell lines *in vitro* and *in vivo*. Our results show that Vγ9Vδ2 T cells exhibit potent antitumor effects against PEL cells and give evidence to support a clinical study of immunotherapy using Vγ9Vδ2 T cells.

The result of blocking studies revealed that Vγ9Vδ2 T cells recognized endogenous mevalonate metabolites and MICA/B of PEL cell lines (Fig. 3B). The recognition of these antigens is considered to exert the difference of cytotoxicity among PEL cell lines. The mechanism responsible for Vγ9Vδ2 T cell killing of PEL cells was via perforin and TRAIL, but not the FasL-mediated pathway (Fig. 3B), although PEL cell lines expressed both Fas and TRAIL-R (Fig. 3A). It has been proposed that v-FLIP, viral analogs of FLIP encoded by HHV-8, binds to FADD and caspase-8, and thereby inhibits Fas-mediated apoptosis [28]. The presence of some decoy receptors, which are related to Fas but lack a functional death domain [29,30], might also influence resistance to death receptor-mediated apoptosis. Although DR4 and DR5 expressing cells are much more in BCBL-1 (8.4 and 3.2 respectively) compared with BC-3 (3.1 and 1.8 respectively) in Fig. 3A, blocking TRAIL caused significant killing inhibition of BC-3 (means of 18.4% inhibition) instead of BCBL-1 (means of 6.2% inhibition) in Fig. 3B. Resistance to TRAIL-induced apoptosis or some decoy receptors might be related to the difference of killing inhibition [14].

Previous studies have shown that CD107a expression on the cell surface is a marker associated with the degranulation of cytotoxic lymphocytes [16,17]. We also confirmed the upregulation of surface CD107a expression on Vγ9Vδ2 T cells following coculture of Vγ9Vδ2 T cells with PEL cell lines (Fig. 4). Our study demonstrates that Vγ9Vδ2 T cells induced efficient apoptosis of PEL cells via the release of cytotoxic granules, and CD107a expression on the cell surface could be a marker associated with the degranulation of Vγ9Vδ2 T cells.

In the present study, we investigated the direct involvement of Vγ9Vδ2 T cells in the growth and invasion of PEL cells using NOD/Rag-2/Jak3 double-deficient (NRJ) mice [18], which displayed rapid and efficient engraftment of PEL cells and Vγ9Vδ2 T cells, as a small animal model. NRJ mice display not only complete deficiency in mature T/B lymphocytes and complement protein but also complete deficiency of NK cells, indicating that they are appropriate recipients of human hematopoietic and tumor cells, as are NOD/Scid/common γ-deficient (NOG) mice [31]. While the efficacy of Vγ9Vδ2 T cells in tumor xenograft mouse models has been described in the immunodeficient mice bearing s.c. or i.v. tumor xenografts [32–37], we evaluated the effect of Vγ9Vδ2 T cells using an orthotopic PEL xenograft mouse model. Transfer of Vγ9Vδ2 T cells to NRJ mice showed significant inhibition of ascites formation as well as organ invasion (Fig. 5). Previously, Lozupone et al. reported that γδ T cells began to be depleted at 24 h and were undetectable in the spleen of the SCID mouse model 48 h after the i.v. administration of γδ T cells [38]. We confirmed that Vγ9Vδ2 T cells were present and persisted in the spleen and peripheral blood of NRJ mice for at least 7 days after the final i.p. administration of Vγ9Vδ2 T cells (Fig. 7A and C). Depletion of NK cell activity has been reported to facilitate the engraftment of human mature T-lymphocytes [39–41], indicating the contribution to the engraftment of Vγ9Vδ2 T cells. Taken together, NRJ mice are expected to be more convenient recipients of both human tumor cells and Vγ9Vδ2 T cell xeno-transplantation.

As previously reported, HAART is able to improve the prognosis of AIDS-related lymphomas [42,43]. Moreover, antiretroviral therapy could provide potential benefits for the treatment of PEL [44,45], indicating the importance of immunocompetence in the treatment of PEL. Considering the immunodeficient status at the onset in HIV-1-infected patients with PEL, induction of Vγ9Vδ2 T cells is expected to be a potent therapeutic approach instead of conventional therapy. Occasionally, the proliferative responses of Vγ9Vδ2 T cells from patients with cancer were impaired [46]. Although Zol and IL-2 treatment has been reported to improve immunocompetence in HIV-1-infected persons by activating Vγ9Vδ2 T cells [47], developing more efficient expansion and administration of Vγ9Vδ2 T cells in patients with malignancy could lead to the clinical use of immunotherapy by Vγ9Vδ2 T cells for a variety of malignancies as well as PEL.

Please cite this article in press as: H. Goto et al., Potent antitumor activity of zoledronic acid-induced Vγ9Vδ2 T cells against primary effusion lymphoma, Cancer Lett. (2013), http://dx.doi.org/10.1016/j.canlet.2012.12.021